Research on Roof Fracture Characteristics of Gob-Side Entry Retaining with Roof Cutting and Non-Pillar Mining in Thick Coal Seam, China

Lei Zhu
China Coal Energy Research Institute
Mengye Zhao (SLFSerena@163.com)
China Coal Energy Research Institute https://orcid.org/0000-0001-5030-262X
Qingxiang Huang
Xi'an University of Science and Technology
Kai Xu
China Coal Energy Research Institute
Yuyi Wu
China Coal Energy Research Institute
Wenzhe Gu
China Coal Energy Research Institute

Research Article

Keywords: roof cutting and non-pillar (RCN-P) mining, roof movement, microseismic monitoring, roof cutting control layer, "Short masonry beam-masonry beam"

Posted Date: May 28th, 2021

DOI: https://doi.org/10.21203/rs.3.rs-484570/v1

Version of Record: A version of this preprint was published at Geotechnical and Geological Engineering on September 8th, 2021. See the published version at https://doi.org/10.1007/s10706-021-01973-y.

Research on Roof Fracture Characteristics of Gob-side Entry Retaining with Roof Cutting and Non-pillar Mining in Thick Coal Seam, China

Lei Zhu[1], Mengye Zhao[1,2,*], Qingxiang Huang[2], Kai Xu[1], Yuyi Wu[1], Wenzhe Gu[1]

[1] China Coal Energy Research Institute Co.,Ltd, Shaanxi Xi'an 710000, China;
[2] School of Energy Engineering, Xi`an University of Science and Technology, Shaanxi, Xi`an 710054,China;
* Correspondence: zhaomengye@chinacoal.com(M.Z); Tel.: +86-186-9130-5618(M.Z);

Received: ; Accepted: ; Published:

Abstract: Based on the S1201-2 large height mining in the 2-2 coal seam of Ningtiaota colliery with on-site microseismic measurement, physical simulation and theoretical analysis methods, this paper explores the rule of roof movement in thick coal seams with roof cutting and non-pillar (hereinafter referred to as RCN-P) mining, so as to obtain scientific and effective theoretical basis for entry support and to summarize the regional structural characteristics and dynamic periodic fracture characteristics. As can be seen from microseismic events, the entry roof is featured by "two zones and one line" along the horizontal direction, namely, the crack generation area, the roof movement area. Additionally, and the obvious lateral breaking of the entry roof on the coal wall is a typical feature of the thick coal seam with RCN-P mining. The roof is vertically divided into "three zones", the crack generation area, the roof movement area and the crack development area. The roof cutting activity mainly affects the overburden activity within the basic roof height range, which is also the roof movement area. In addition, the distribution frequency and the intensity of microseismic events indicate the roof periodic breaking characteristics. The "breaking pressure relief," "advanced crack development," and "the limit breaking state" of roof breaking corresponds to the initial, middle, and final stage of breaking in the periodic weighting process, respectively. Compared with the normal mining, the RCN-P mining reduces the periodic weighting length and increases the pressure strength. As is shown in the physical simulation experiment, the basic roof and the cutting control layer in the "regional structural characteristics" constitute the "large" and "small" structures with RCN-P mining. The basic roof key layer is the core to control the stability of the strata, and the breaking process from the cantilever beam to the short masonry beam of the roof-cutting control layer is the main cause of the entry stress. Correspondingly, the basic structure model of "short masonry-hinged" roof was proposed and the calculation method of support was established for the entry with RCN-P mining in thick coal seam, providing a research foundation for scientific and effective rock formation control.

Key words: roof cutting and non-pillar (RCN-P) mining; roof movement; microseismic monitoring; roof cutting control layer; "Short masonry beam-masonry beam";

1. Introduction

Gob-side entry retaining with RCN-P mining is an efficient and green coal mining technology[1,2]. With only one or without the entry needs to be excavated at a working face to achieve complete recovery of coal pillars[3,4]. Non-pillar mining sets off the protective effect of the section coal pillars, which leads to the stability of the surrounding rock closely related to the breaking of the roof movement[5,6]. Due to the lack of support on one side of the pillar, the basic surrounding rock structure[7,8] composition of the entry has changed[9], as a result, the roof movement law cannot be applied in accordance with the tradition[10,11].

Manchao He proposed an innovative coal non-pillar longwall mining method[12,13]. The mechanical model is established and the mechanism of the new method is discussed. A directional roof fracturing technique to promote roof caving in goaf is proposed. Constant

resistance and large deformation anchor cable (CRLDA) are used to stabilize roof of entry. Field monitoring shows that the reserved items are stable, which meets the actual needs of field mining[14]. Jinzhu Hu et al. established the mechanical model of roof cutting of GERRC, and pointed out that the depth and angle of roof cutting were the key parameters, and analyzed the reinforced concrete at different depths and angles[15]. Xiao Liu et al. analyzed the stress characteristics of the goaf, and introduced the equivalent concentrated load in entry. The mechanical model of roof cutting support is established, and the applicable scope and key parameters of determination method are analyzed[16,17]. Nong Zhang et al. analyzed the stability of goaf retaining entry along goaf in four stopes in China and evaluated the influencing factors of entry deformation, such as mining depth, support strength, and mining depth. On the basis of continuous superposition, the supporting resistance model of the side wall of the filling goaf is derived[18,19]. Lifeng Li et al. verified the model parameters through the measured leading abutment pressure and numerical calculation, and studied the energy density in the mining process. The failure of the lateral abutment energy supports body of the adjacent working face, and the large deformation of surrounding rock often occurs in goaf side entry under the influence of multiple energy disturbances[20,21].

However, the selection of on-site support mostly relies on on-site experience and lacks the corresponding theoretical basis, especially the related research on roof failure characteristics. Therefore, based on the research traditional roof structure and overburden movement[22,23], by means of microseismic monitoring[24-27], the breaking process of entry with RCN-P is monitored on site to clarify its breaking process and structural form. Being both theoretically and practically significant, the research results can provide references for the mechanism of entry failure, the relationship between "support and surrounding rock", the selection of support equipment, the design of entry retention parameters and the optimization of entry retention process.

2. Engineering background

2.1.Overview of the Research Area

The colliery of Ningtiaota is one of the three pairs of super large mines invested and constructed by Shaanxi Coal chemical Industry Group Company in the south of Shenfu mining area. The mine design production capacity is 12.00MT/a, and the approved production capacity is 18.00MT /a. Ningtiaota colliery is the first mine in China that realized the technology of non-pillar and roof cutting mining with large mining height[28]. For a better study of the characteristics of roof breakage under non-pillar roof cutting, on-site microseismic monitoring was carried out on the mining face of S1201-2 Ningtiaota colliery.

The mining face of S1201-2 is located in the south No.1 panel. The mining face is reserved for S1201-3 in the west and S1201-1 mined in the east. The mining face layout is shown in Figure 1. The main mining face is 2^{-2} coal seam, based on the data in the study area and surrounding boreholes, the average thickness of 2^{-2} coal seam is 4.33m.

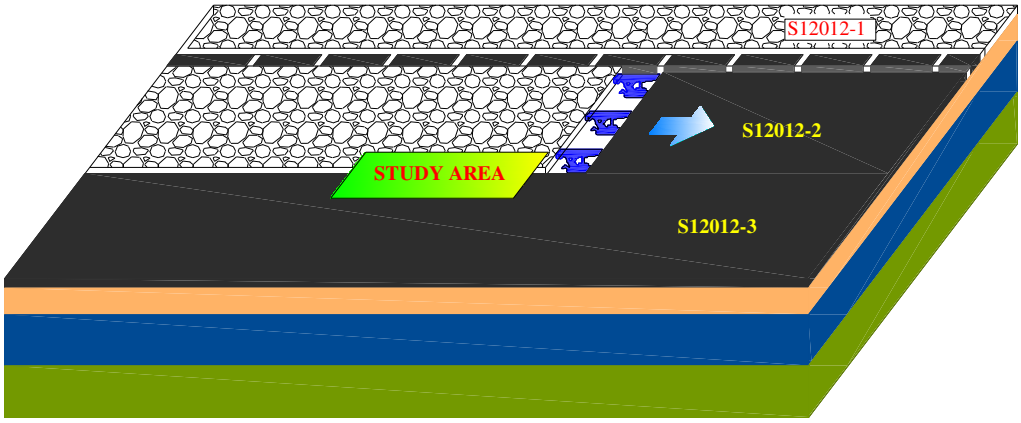

Figure.1 Study area layout

2.2. Entry support

In the process of RCN-P mining, the entry goes through multiple stages, such as primary mining, primary mining stability and secondary mining. The surrounding rock deformation of the entry is considerable and long lasting. "Anchor cable + plastic steel mesh" is used to support the roof on site. The coal side adopts the support of "fiberglass bolt + lead wire mesh". The gravel side is supported by "wavy bolt + steel mesh", as shown in Figure 2.

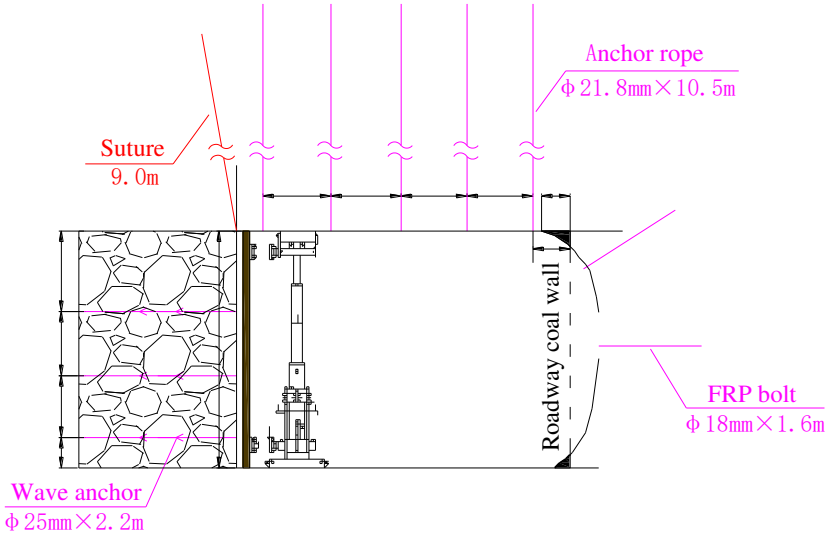

Figure.2 Layout of entry section

1) Surrounding rock supporting

Five anchor cables are arranged in each 800mm spacing row of the remaining entry. Length: 10.5m, diameter: 21.8mm. The pre-tightening force is 28T, and a W steel strip with a length of 2.0m is used to connect every 3 anchor cables along the entry with constant resistance. Arranged variously, the coal side adopts the support of "fiberglass bolt +8# lead wire mesh". The length of the bolt is 1.6m and the diameter of the bolt is 18mm.

2) Temporary reinforcement of roof support

During the advancing process of the mining face, a certain range behind the mining face is the main area where the roof moves, resulting in severe deformation of the surrounding rock of the entry, which requires key control. According to the law of appearance of mine pressure on site, the unit support is used to temporarily strengthen the support behind the mining face.

3) Caved gangue support

The control effect of gangue caving in the goaf determines the effect of entry retention. The roof rock gradually collapses as the mining face is mined. Method of unit support + U-shaped steel +

metal mesh is adopted in order to prevent the crushed rock slab from bulging into the lane when it is not compacted and instable, and to enhance the stability of the collapsed gangue and improve the control effect on the roof structure.

3. Analysis of Microseismic Field Measurement of Roof Movement

3.1. Monitoring system establishment

This study explores the roof movement process by means of microseismic monitoring. Microseismic monitoring monitors the generation, expansion, and internal energy accumulation of cracks in the rock during the friction. It propagates in the form of P and S waves and accurately determines the time, location, and magnitude of the microseismic event in the rock mass (real-time air strength), so as to make a qualitative and quantitative evaluation of the activity range, stability and development trend of the rock mass damage.

1）Measuring point layout

The S1201-2 mining face of Ningtiaota colliery adopts the mining method of RCN-P, so that the entry is retained to serve the S1201-3 mining face. The exploration area is located in the belt along the groove near the stop line, and a group of microseismic sensors are arranged at every 30m. The sensor is arranged in the roof stable rock formation in a manner that follows the mining. On-site detection is based on the positioning principle and the sensor is designed to be vertically arranged on three layers , the sensor layout is shown in Figure 3 and 4, the drilling construction is shown in Figure 5, and the parameters are shown in Table 1.

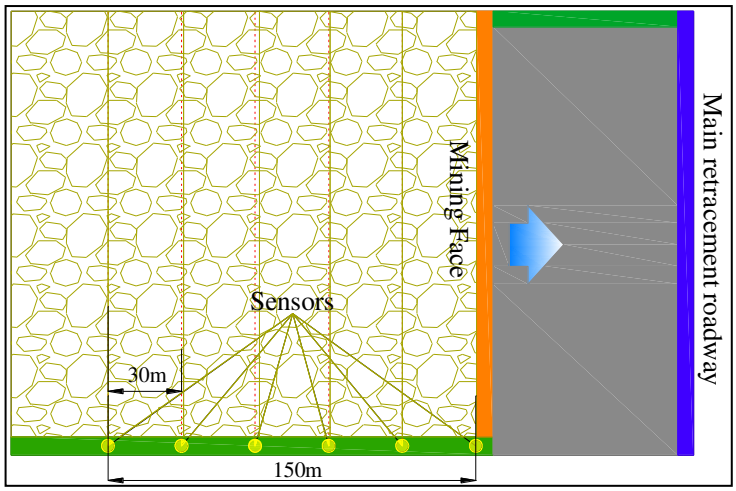

Figure.3 Top view of microseismic sensor measuring point layout

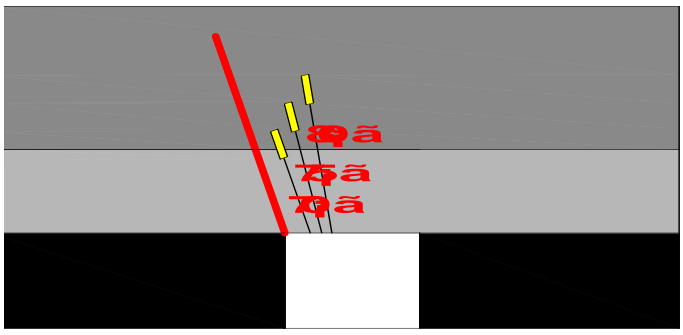

Figure.4 Side view of microseismic sensor layout

Figure.5 Drilling installation construction

Table 1. Drilling parameter design

Number	Design depth (m)	Measured depth (m)	Design inclination (°)	Measured inclination (°)	Design aperture (mm)	Measured aperture (mm)
1#	5	4.97	70	69.8	50	49.5
2#	7	6.96	80	79.1	50	48.7
3#	6	5.88	75	75.8	50	48.7
4#	5	4.96	70	68.7	50	48.6
5#	7	6.97	80	79.8	50	47.9
6#	6	5.95	75	75.4	50	49.4

2）Monitoring process

The microseismic monitoring system mainly includes: sensors, paladin digital signal acquisition system, ground host processing system, transceivers, cables, optical cables, and junction boxes. The ground host is placed in the wellhead fleet office, and the digital signal acquisition system is transported to the S1201-2 retracement window (Figure 6) by a rubber wheeled vehicle.

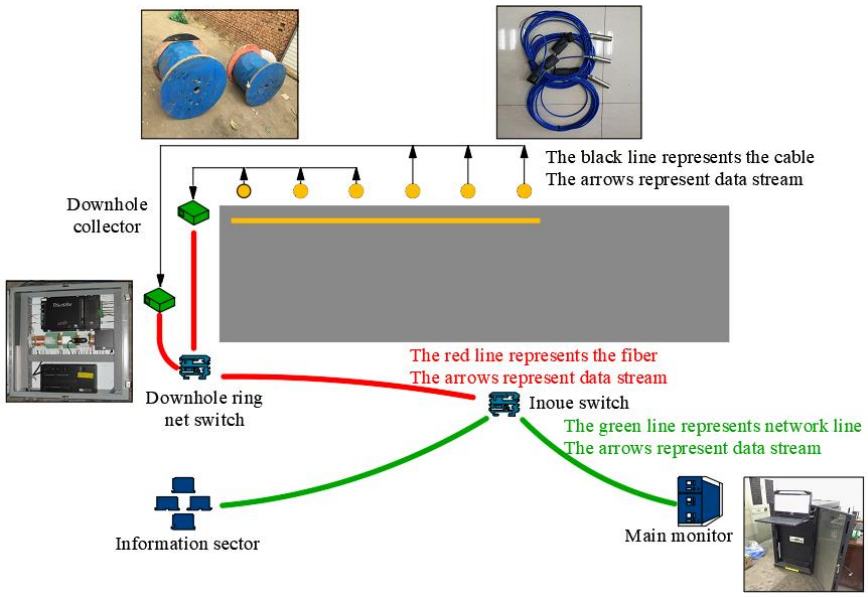

Figure.6 Communication Line Layout

3）Run test

① Host and sensor parameter setting

System and sensor parameter setting are the main task of ESG system debugging.

② Establishment of microseismic waveform database and filtering processing

Underground noise varies widely. Even the same kind of noises have different characteristics because of different conditions and environmental factors. It is necessary, therefore, to deal with all kinds of underground noises. Only by performing full waveform analysis can their characteristics and changes be accurately grasped.

During the test, each type of noise was repeatedly analyzed, summarized and classified, and a database of underground noise signals and AE acoustic emissions suitable for Caragana mine were established (as shown in Table 2). Among them: the X-axis in all the following waveform diagrams signifies time (ms), and the Y-axis refers to the amplitude value, that is, the output voltage (v).

Table 2. Typical waveform signal

The name of the noise	Waveform figure	The name of the noise	Waveform figure
Standard microseismic waveform		Coal cutter Operation	
Underground operation vehicle passing	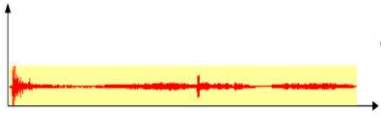	Rubber wheel truck loading, unloading	
Blasting of roof cutting	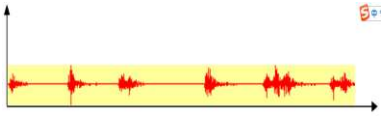	Water flow hits rock mass of entry	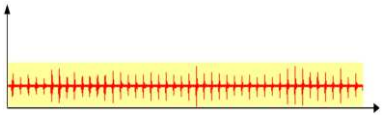
Effective AE signal after roof cutting	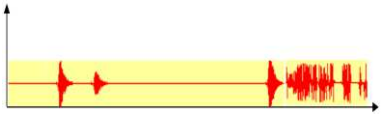	Metallic impingement rock	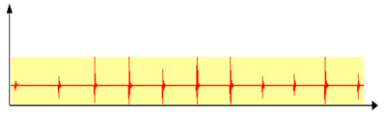

It can be seen from the above listed waveform diagrams that the characteristics of various signal waveforms caused by different reasons, and most of the waveforms have a short duration, ranging from tens to thousands of milliseconds.

The signal duration is the shortest when hitting metal objects, such as bolts inside the rock mass and the surrounding rock of the entry, generally about 10ms;

The passing signal of the minecart is a long interference signal, generally as long as about 1min, which can be clearly distinguished;

The vibration caused by the rotation of the fan does not have much regularity with the loading and unloading signal of the mine car, and the amplitude is not the same;

The regularity of the impact of the water flow from the roof drain hole on the entry rock mass is obvious;

The signals generated by roof cutting energy blasting and percussion on the surrounding rock mass of the entry are generally regular, and the amplitude of each vibration waveform is roughly the same. In addition, the duration is very short, and the coda is not fully developed;

The above list is only the typical waveform signals monitored since the operation of the system. With the continuous improvement of monitoring data, the types of waveform signals obtained will be complete. Comparison of the characteristics of various signals.

The entire preparation, installation, commissioning, monitoring and analysis work spanned over one year from May 2018 to May 2019. The specific monitoring work completed is shown in Table 6.

3.2 Analysis of characteristics of microseismic events during roof failure

1）Distribution characteristics of microseismic events

From December 13, 2018 to January 10, 2019, continuous on-site monitoring of microseismic events with an elevation of 1285m and a strike length of 180m was performed on the S1201-2 mining face of Ningtiaota colliery. During the microseismic monitoring period, 2,875 monitoring data were collected. The distribution of microseismic events is shown in Figure 7. The sphere in the figure represents the micro-rupture of the overburden of the mining face. The shape of the event indicates the energy of the event. The larger the shape of the event, the greater the energy. The change in color indicates the magnitude of the moment magnitude. With the color changing from purple to yellow, the moment magnitude gradually increases.

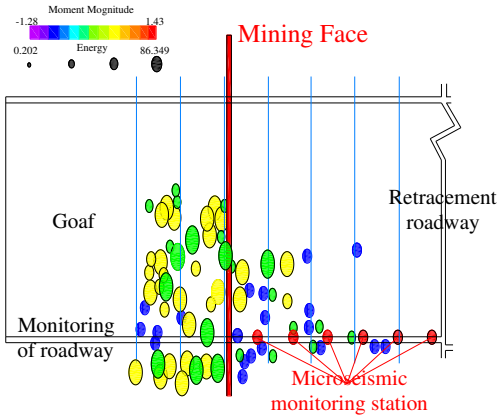

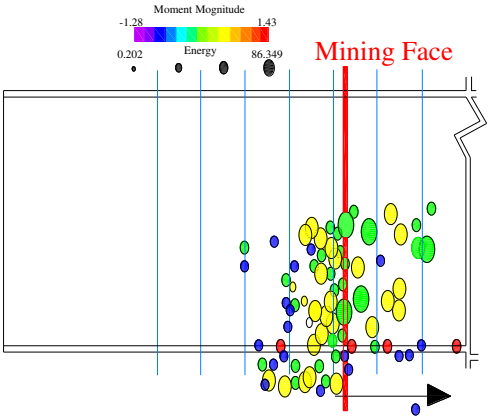

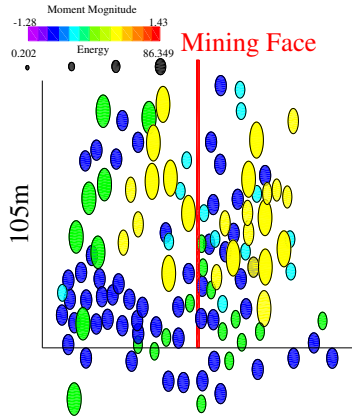

（a）Mining face advance 10m

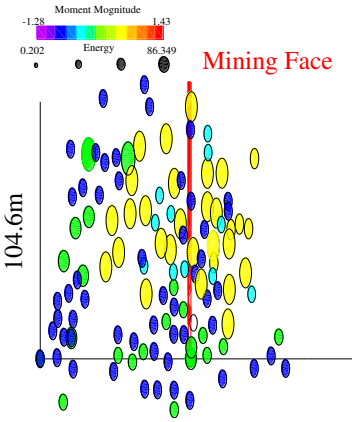

（a）Mining face advance 21m

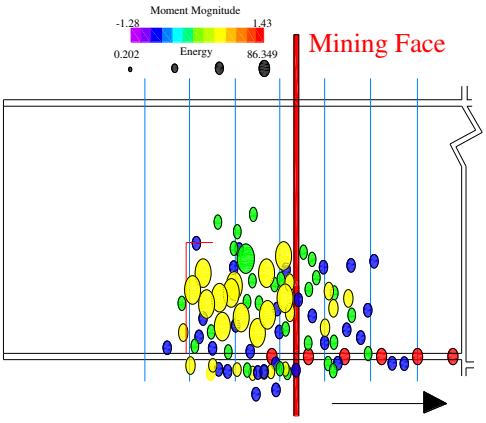

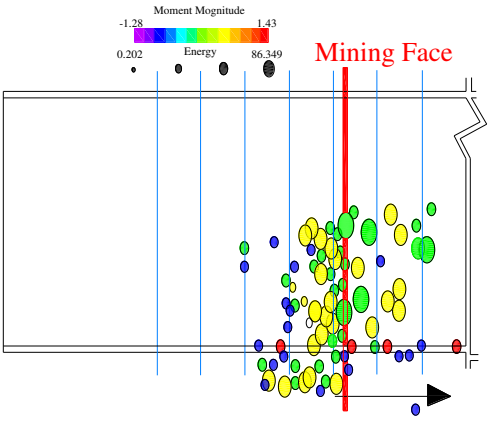

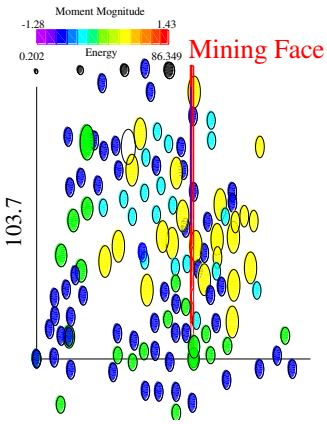

(c) Mining face advance 30m

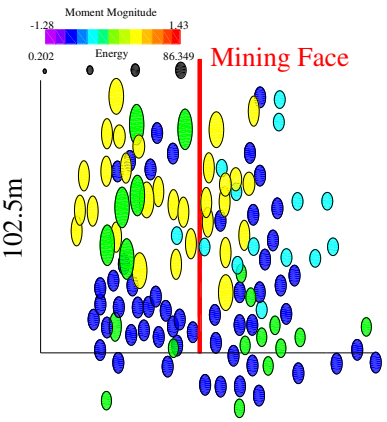

(d) Mining face advance 44m

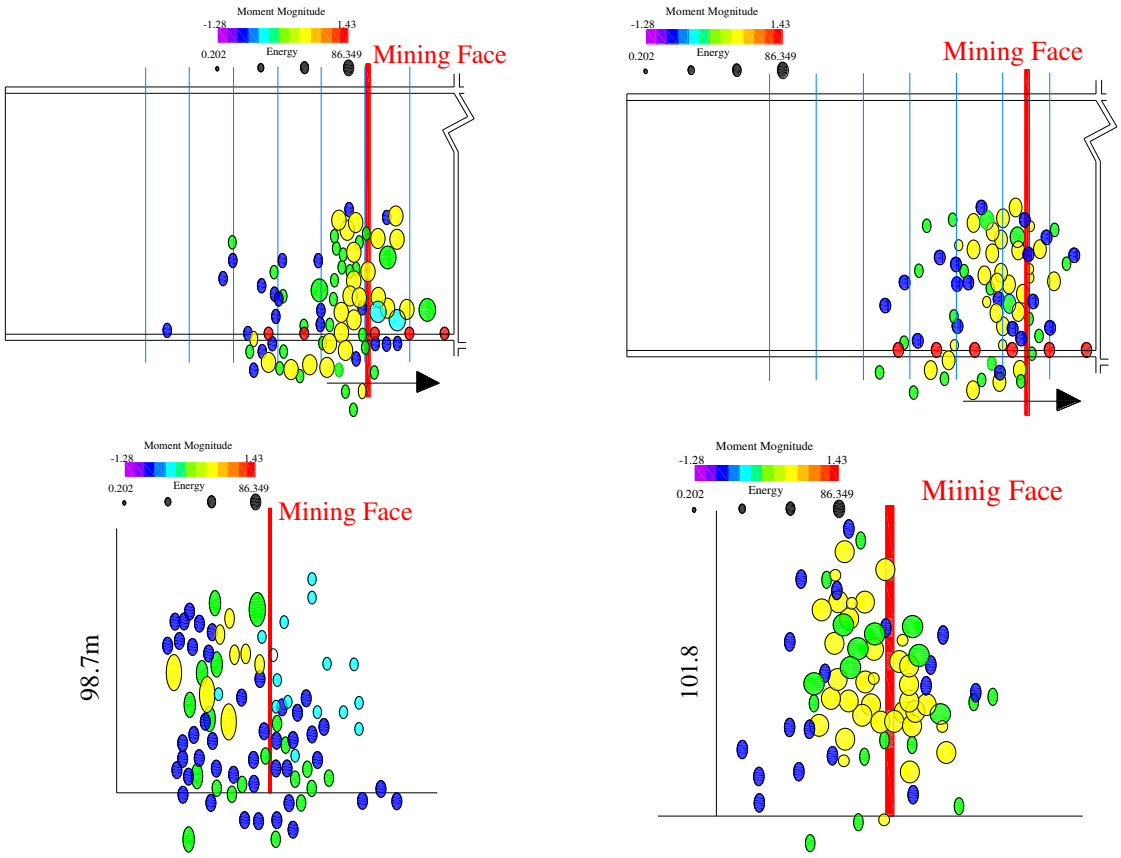

(e) Mining face advance 123m (f) Mining face advance 135m

Figure.7 Distribution characteristics of microseismic events at mining face

The statistical results are shown in Table 3.

Table 3. Microseismic event distribution data

Mining face position	Number of microquakes	Vertical distribution range (m)	Leading distribution range(m)	Lag distribution range (m)	Influence area of coal wall side (m)
Advance 10m	174	25~80	0~24	0~45	7
Advance 21m	247	21~85	0~20	0~40	8
Advance 30m	247	19~79	0~19	0~32	8
Advance 44m	247	19~84	0~18.4	0~34	12
Advance123m	177	22~80	0~16.7	0~43	11
Advance135m	185	19.7~85	0~19.4	0~41	6

2) Horizontal distribution characteristics of microseismic events

The horizontal distribution characteristics of microseismic events were analyzed (Figure 8) during mining. The farthest end of the microseismic event concentrated area of the leading face was between 15~24m from the mining face, the concentrated lagging mining face of which was at the mining face. Microseismic events were always concentrated within the range of 31~45m behind the mining face, and the roof overlying rock movement is relatively active.

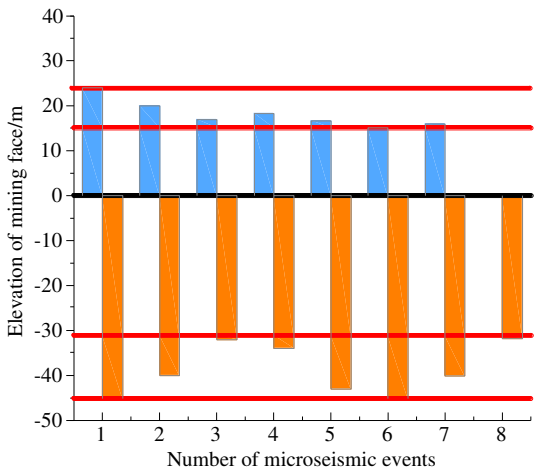

Figure.8 The impact range

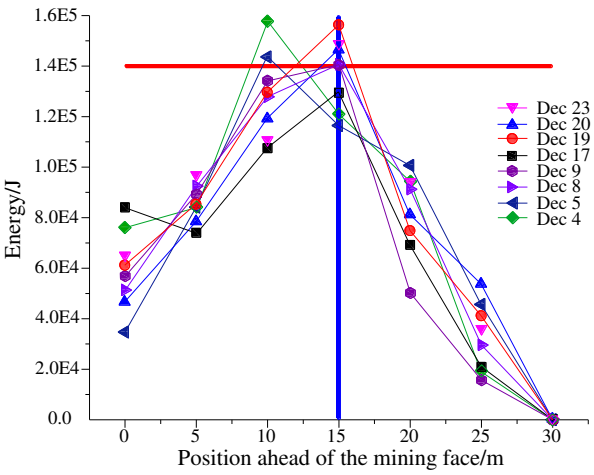

Figure.9 Energy distribution curve

Statistics and analysis of the microseismic events (2875 in total) in the microseismic area affected by the motion were carried out, and the cumulative energy value of the microseismic events was suppressed according to the period that was taken as the threshold value to judge whether the rock formation has been damaged to the fracture. The maximum accumulated energy of microseismic events in different areas of the leading mining face exceed the threshold 1.4E+05 Joule. The mining face corresponding to the mining face was mined. The cracks in this area were derived from a large number of microfractures into macro cracks. According to the microseismic statistical results (as shown in Figure 9), within the range of 10~15m from the advanced mining face, the roof gradually formed a macroscopic fracture, which conformed to the basic law of advanced fracture of the roof.

Taking the microseismic event from the mining face to 30m (Figure 7(c)) as an example, the analysis shows that the horizontal distribution of the microseismic event has obvious regional characteristics. According to the energy and density of the microseismic event, the groutable roof is divided into the crack generation area and the roof movement area. In addition, the lateral breaking position of the roof can be determined along the inclination direction.

① Crack generation area

15~25m ahead of the mining face is the generation area of roof cracks. The density and energy of microseismic events in the area are generally low. The roof is dominated by the generation and development of microcracks. The distribution of microseismic events presents asymmetrical characteristics. The position of the entry gradually decreases to the middle of the mining face.

The mining face is 10~15m ahead, the energy exceeds the threshold, and the roof has obvious macroscopic cracks, which is the area where the roof is broken in advance. There is no obvious roof movement in this area, and the development of fissures is dominant.

② Roof movement area

The density and energy of microseismic events within the range of 0-32m behind the mining face have greatly increased, and the roof movement characteristics are obvious. From the position of 30m behind the mining face, the density and intensity of microseismic events have been significantly reduced, and the roof movement tends to be stable.

③ Lateral breaking position

This is an important parameter of the roof movement characteristics at the lateral breaking position of the roof when the roof is cut without coal pillars along the goaf. The monitoring results show that the microseismic events on the coal wall side of the entry have a distribution range of 6~12m, of which the microseismic events at 6~8m are linearly distributed, with high concentration and greater energy than the macro breaking energy standard. This position is the lateral breaking position of the entry roof.

3) Vertical distribution characteristics of microseismic events

To take the vertical distribution characteristics of microseismic events from the mining face to 30m as an example (Figures 10 and 11), the distribution of microseismic events has obvious regional characteristics and can be divided into fracture generation area, roof movement area and fracture development area.

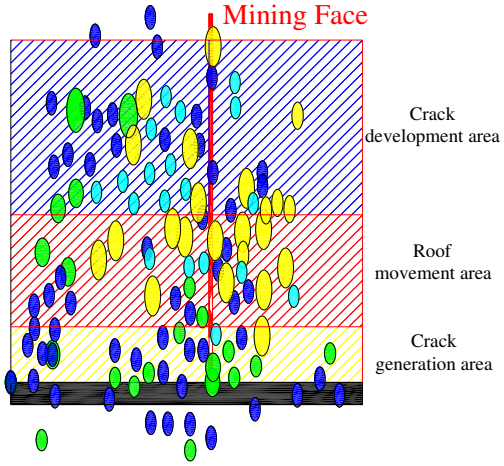

Fig.10 Vertical distribution characteristics

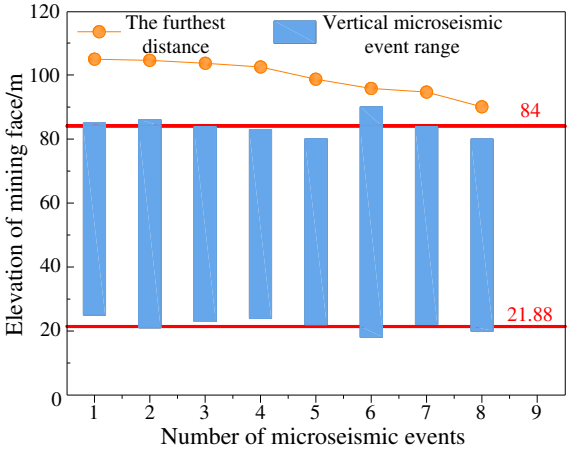

Fig.11 Vertical concentration range

① Crack generation area

Within the range of 0-12m above the roof of the entry, the density and energy of microseismic events are low, and there is no obvious macroscopic fracture, and the cracks are the main cause. This height is mainly the range of roof cutting height. The roof cutting effect cuts off the interconnection between the roofs. The roof of the entry remains relatively stable without significant breakage and movement. This is the main feature of the overburden failure of the roof with RCN-P mining.

② Roof movement area

The range of 21~45m above the entry is the roof movement area. At this stage, the density and energy of microseismic events have greatly increased. By the criterion of the energy of microseismic events, macroscopic cracks develop. This range is mainly the main height range of the basic roof movement.

③ Crack development area

The 45-84m above the entry has a high concentration of microseismic events, but the energy is less than the macro-breaking energy standard. It is mainly based on the development of fractures. This height range is the height of the fracture zone of coal mining, so this area is a fracture development area.

The above analysis results show that, according to the spatial structure distribution characteristics of microseismic events, the entry roof can be horizontally divided into "two zones and one line" , that is, the crack generation zone, the roof movement zone, and the lateral secondary breaking line. 10~15m ahead of the mining face is the area where the leading cracks are generated. The breaking movement of the roof is concentrated in the range of 30m behind the mining face. The roof of the entry is likely to be laterally broken 6-8m inside the coal wall of the entry, and the roof above the entry is obviously broken. The lateral fracture of the thick coal seam is a typical feature of the horizontal fracture of the roof of the thick coal seam with RCN-P mining.

3.3 Periodic breaking rule of roof

The regularity of microseismic distribution was strong when the mining face was advanced from 106.4m to 165.9m, as shown in Figure 12.

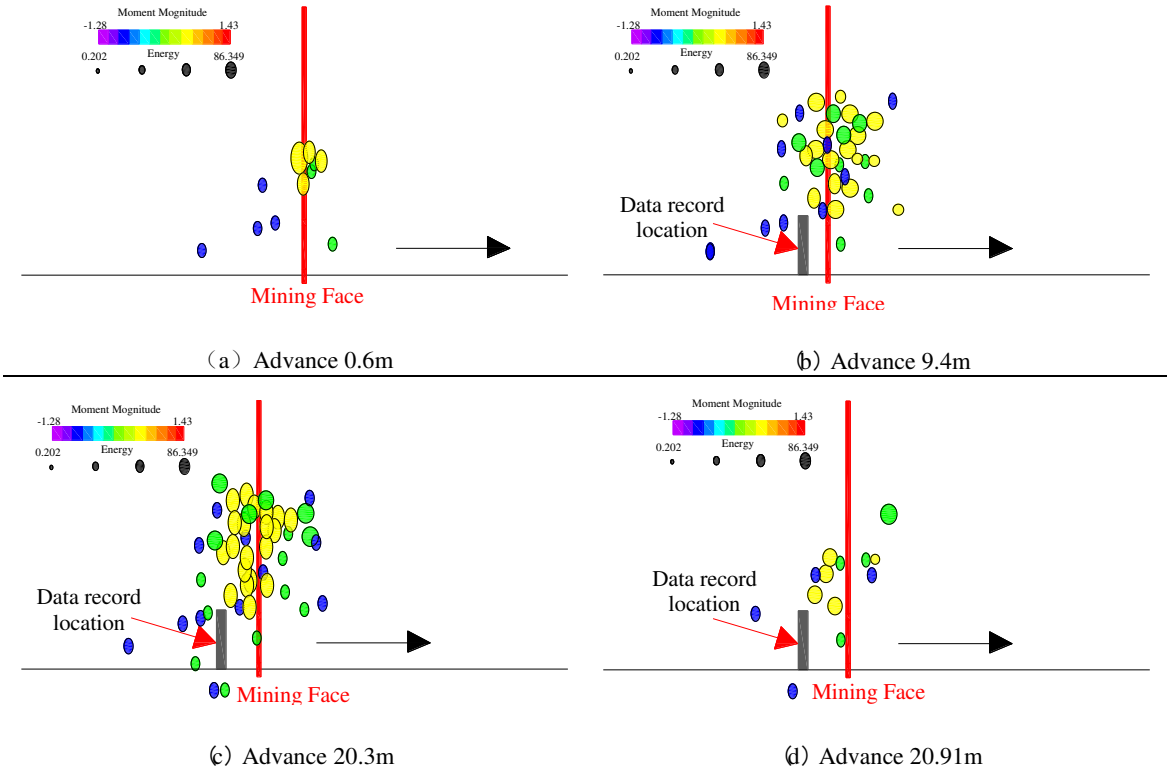

Figure.12 Period distribution characteristics of microseismic events

During the mining process, the microseismic event of the entry roof changed periodically with an average period of 2 days. At the beginning, there were few microseismic events and low energy. As the exploitation continued, the number of microseismic events gradually increased and the energy was high. When the mining reached a certain distance, the number of microseismic events reached the peak, and the event energy was the highest. Subsequently, the microseismic events decreased sharply, and the high-energy microseismic event disappeared quickly. The mining process of the mining face repeated the above-mentioned periodic process.

Through the microseismic monitoring of 3 complete cycles of pressure on the 2^{-2} coal 4.0m large mining height with RCN-P mining of Ningtiaota colliery, the microseismic events showed periodic changes. According to the distribution characteristics of microseismic events, their cyclical development can be divided into the initial period, the middle period and the end of cyclical recovery. The monitoring data showed that when the mining face was in the initial period of 0.6m, 20.91m and 40.43m, the system monitored 11, 10 and 8 microseismic events, respectively. When the mining face was at 9.4m, 30.01m, and 50.01m in the mid-cycle mining, the system monitored 74, 68, and 73 microseismic events, respectively. When the mining face was 20.3m, 39.81m, and 59.61m at the end of the period, the system monitored 196, 185 and 179 microseismic events.

Based on the above content, the periodic development process of microseismic events can be summarized:

① In the initial stage of the period weighting, the previous period of mining had just ended, the roof had undergone a process of breaking and pressure relieved. The development of microseismic events near the mining face was low and mild, and only a few microseismic events were distributed about 17m ahead.

② In the mid-period stage of the period weighting, when the mining face was mined to a position of 9.4m, there was a concentrated microseismic event 14m ahead of the mining face. The microseismic event was mainly vertically distributed in the range between 21.56m to 70.23m. Under normal circumstances, this area was easy to form advanced macroscopic cracks. In the subsequent mining process, the frequency and intensity of microseismic events in this area had greatly increased,

and vertically extended to a higher level, and the advanced macroscopic cracks had further intensified.

③ In the final stage of the period weighting, when the mining face was mined to 19.46m, the distribution range, intensity and frequency of microseismic events had reached the maximum, the macroscopic fractures developed to the greatest extent, and the basic roof reached the limit breaking state.

The results of the microseismic monitoring were drawn into the curve as shown in Figure 13. The analysis showed that the average weighting length was the 18.74m in the RCN-P mining area, and the value in the middle area of mining face was 18.76m.

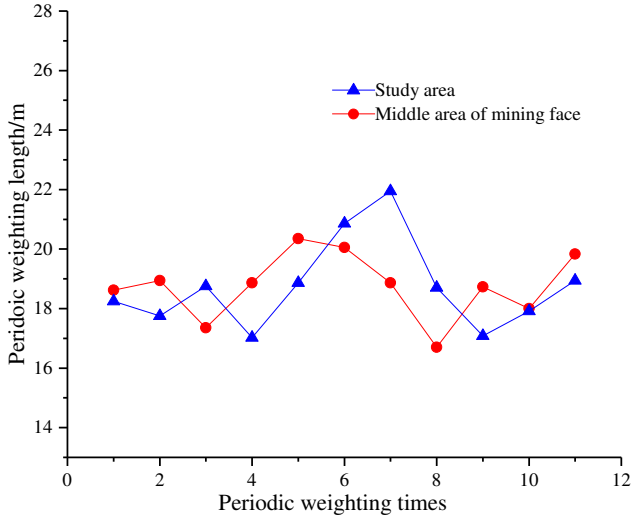

Figure.13 Periodic weighting length of microseismic monitoring

In addition, through manual on-site monitoring, the periodic weighting length and intensity in the same period of time are counted. The data was shown in Table 8.

Table 8. The statistics of periodic weighting length and strength

	Normal mining area		Middle area of mining face		RCN-P mining area	
Periodic weighting times	**Strength (MPa)**	**Periodic length (m)**	**Strength (MPa)**	**Periodic length (m)**	**Strength (MPa)**	**Periodic length (m)**
1	29.24	15	38.6	17.3	39.2	15.9
2	31.6	16.3	36.9	14.8	36.4	17.4
3	28.6	15.8	38.6	18.9	37.4	21.3
4	29.3	20.3	37.7	26	36.5	22.9
5	32.6	24	37.4	25	37.5	23
6	35.7	24.8	37.5	24.7	38.9	24.7
7	39.8	19.6	38.2	23.1	34.9	15.7
8	34.7	15.6	38.1	17	35.6	21.4
9	35	17	39.5	18.2	36.8	16.9
10	37.6		37.9	18.9	37.6	15.6
Average value	33.41	18.71	38.04	20.39	37.08	19.48

As shown in the on-site statistics, the average period length of the study area was 18.16m. The average period length of microseismic monitoring was 18.74m. It can be seen that the periodic breakage of the roof was consistent with the periodic development characteristics of roof microseismic events, which fully demonstrated the accuracy of microseismic monitoring.

Compared with the normal area on the other side of the mining face, the RCN-P mining reduced the periodic weighting length by 10.2%, and the pressure strength was increased by 11%. The graph is shown in Figure 13, data is shown in Table 8.

4 Physical similarity simulation analysis of roof movement

Gob-side entry retaining with RCN-P mining is affected by repeated mining on both sides of the mining face, and the roof structure of the entry is in a dynamic process of change. The evolution process of entry roof deformation and failure is mainly as follows: The mining disturbance at this mining face increases the stress of the surrounding rock of the entry →The roof slews down to the side of the goaf →The shallow surrounding rock is broken and the deep cracks increase →Basic roof breaks along the lateral side →The load of the supporting body increases and the deformation speed of the surrounding rock accelerates →The entry roof rotation subsidence further intensifies until it stabilizes →The entry continues and slowly deforms after the primary mining ends →The stress of the surrounding rock of the entry increases →The stress of the surrounding rock of the entry increases when the next mining face is mined →The entry is completely destroyed after mining.

4.1 Simulation experiment design

In the process of gob-side entry retaining with RCN-P mining, the mining conditions such as roof cutting parameters and mining height directly determine the breaking rule of the roof. In order to further reveal the rules of the roof movement of the entry without coal pillars, a physical similarity simulation experiments were carried out. The mining height was 4.3m, the roof cutting depth was 9m, and the roof cutting angle was 15°.

Based on the effect of roof cutting, the model design can maximize the observation of the failure movement of the roof cutting control layer (in the range of the roof cutting height) and the basic roof. Considering the effect of buried depth, load transfer and stress similarity ratio, the load effect on the upper part of the entry can be achieved by manual loading. The simulation experiment model had a width×height×thickness of 120cm×80cm×20cm, a geometric similarity ratio of 1:50 (satisfying full mining on the goaf side), a bulk density similarity ratio of 1:1.5, and a stress similarity ratio of 1:75. According to the stress similarity ratio, a uniform load of 0.2 MPa was applied to above the physical model, as shown in Figure 14.

Figure.14 Physical simulation panorama

4.2 Simulation analysis of roof breaking process

1) Initial breaking stage of roof

Before excavation, the roof on the side of the entry close to the mining face was cut. The initial load is uniform, and the original rock stress on the roof was simulated. In order to truly simulate the mining environment on site, the excavation was carried out quickly from left to right as shown in Figure 15.

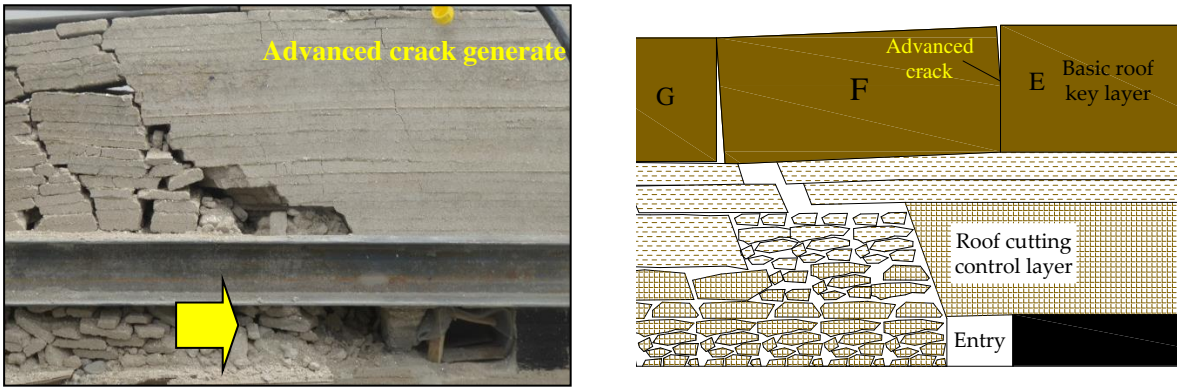

(a) Similarity simulation experiment results (b) Structural diagram

Figure.15 Triangular arch structure of Basic roof

After the mining face excavation, the rock mass in the side goaf of the entry collapsed immediately, and the rock mass at the position of roof cutting was greatly broken. The roof cutting control layer formed a stable "short cantilever" structure. The key layer of the basic roof was broken in advance above the entry, turning and sinking toward the side of the goaf, and was hinged with the broken rock mass in the goaf to formed a hinged structure. The breaking angle of the basic roof key layer is 75°, and the limit breaking distance was 11.4m. The movement of the roof overlying strata at this stage was mainly due to the fracture of the basic roof key layer to form a lateral triangular arch structure.

2) Roof movement stage

There was a continuous loading on the roof above the entry to simulate the force of the overlying surrounding rock. The rotation and subsidence of the basic roof key layer became more intense, so did the breaking and cracks on the entry roof. Under the force of the basic roof key layer, the roof cutting control layer broke along the coal wall of the entry, forming a conductive crack between the break line of the cutting roof control layer and the basic roof, and resulting in a 3° rotation and cutting-off along the coal wall of the entry. The movement of the roof overlying rock at this stage was mainly due to the development of vertical fractures, which eventually penetrated the roof cutting control layer, forming conductive cracks on the roadside coal wall, as shown in Figure 16.

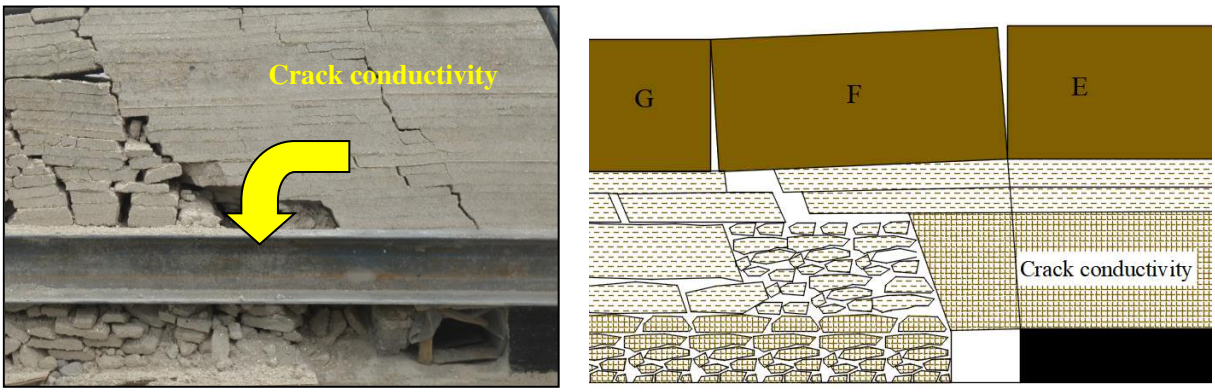

(a) Similarity simulation experiment results (b) Structural diagram

Figure.16 The roof cutting control layer breaking

3) Stabilization stage of the roof

Stress was loaded to simulate the forces on the entry during the advance mining of the next working face, the entry roof cracks fully penetrated. The basic roof key block and the broken rock mass in the goaf formed a "masonry beam" structure and remain stable. The roof cutting control layer was cut off along the coal wall and formed a "short masonry beam" structure with the rock

mass in the goaf. With the entry severely deformed and subjected to high roof pressure, the cut-off damage of the combined roof along the coal wall was the most dangerous form of RCN-P mining. With the entry severely deformed and subject to high roof pressure, the cut-off damage of the combined roof along the coal wall was the most dangerous form of RCN-P mining. In the field mining, the single-form pillars used in the entry were often crushed and the rotation characteristics of the roof were clearly seen, indicating the high stress in the roof and the reliability of the simulation phenomenon.

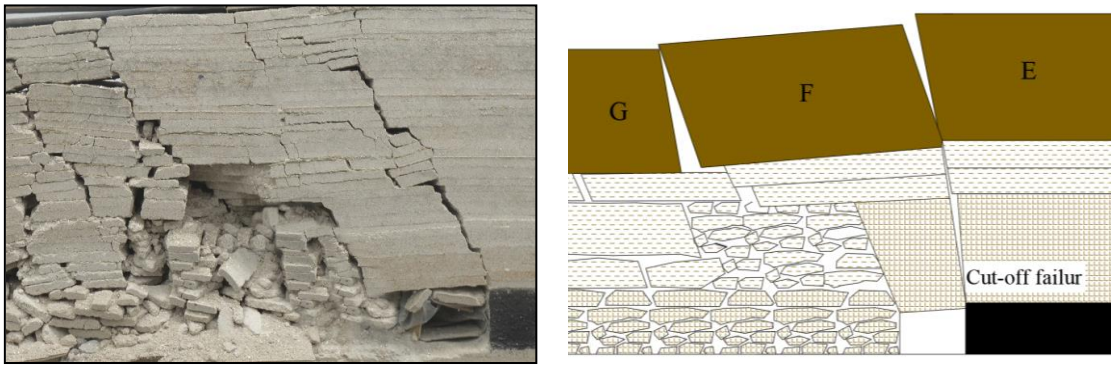

(a) Similarity simulation experiment results (b) Structural diagram

Figure.17 Cut-off failure of roof

As indicated by the simulation experiment results, the key layer of the basic roof and the control layer of the cutting roof respectively constitute the "large" and "small" structures with RCN-P mining. The stability of the breaking structure of the basic roof key layer is the key to controlling the rock formation, and the breaking process from the “cantilever beam” to the “short masonry beam” of the roof cutting control layer was an important reason for the force in the entry.

The main purpose of control is mainly to prevent the roof from cut-off breaking during the RCN-P mining process. The control method is divided into two parts: ensuring the stability of the roof cutting control layer and the basic roof fracture structure. Through this method, the roof cutting control layer does not break or breaks at the stable position inside the roadside coal wall, and a stable articulated structure can be formed after destruction. On the other hand, the basic roof fracture structure can support the load of the overlying rock layer, and reduce the stress transmission of the lower strata.

In addition, the stability of the roof structure of the thick coal seam with RCN-P mining was closely related to the cutting height. Shorter cutting roof height indicated less thickness of the control layer of cutting roof. As a result, the "small structure" had a weaker load support capacity. When the roof cutting height is large, the thickness of the top cutting control layer is increased, and the support capacity is enhanced, which effectively realizes the bearing of the overlying rock mass. At the same time, the fragmentation and expansion effect of the cut rock mass are fully exerted, which is more conducive to maintaining the stability of the basic roof key layer.

4.3 Roof structure

The roof structure of RCN-P mining was composed of the roof cutting control layer and the basic roof key layer. The results of physical similar simulation experiments showed that the breakage of the basic roof key layer would cause the structural instability of the short cantilever beam of the roof cutting control layer. When the stress of the cutting roof control layer was greater than its own strength, the roof is easy to break in the inner position of the coal wall of the entry. The main form of breaking was rotary breaking. One side of the broken key block was hinged with the stable roof of the inner coal wall, the other side was hinged to the rock mass cut in the goaf, forming a "short masonry beam" structure of the roof cutting control layer.

1) "Short cantilever beam - masonry beam" structure

With the mining of the working face, the basic roof key layer was broken above the entry. The key blocks E, F and G were hinged to each other after the roof broke. The roof cutting control layer within the range of cutting height did not break, hence forming a short cantilever structure. The structure of the basic roof key layer and the roof cutting control layer is masonry beam and short cantilever beam, respectively, which can be called "short cantilever beam-masonry beam" (Figure 18).

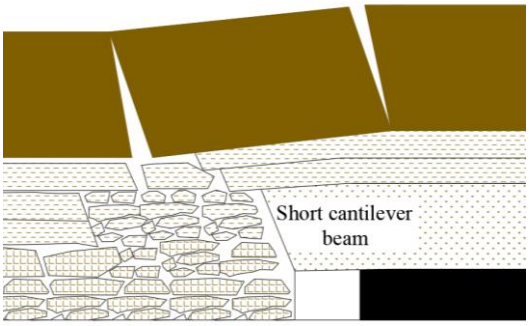

Figure.18 "Short cantilever beam - masonry beam" structure

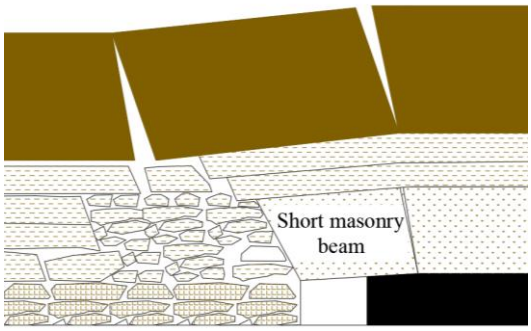

Figure.19 "Short masonry beam - masonry beam" structure

2) "Short masonry beam-masonry beam" structure

The "short cantilever beam-masonry beam" structural form was a temporary structural during the movement of the roof. With the continuous action of the surrounding rock stress, the roof broke along the weak surface of the crack under the action of the roof periodic breaking. After the basic roof key layer was broken, E, F and G were hinged to each other in the form of masonry beams. Under the action of the “large structure” of the basic roof, the roof cutting control layer broke the original short masonry structure and forms H rock block. The breaking location was inside the coal side of the entry. This basic roof key layer formed a masonry structure, and the cutting roof control layer formed a masonry structure. The structure was generally called "short masonry beam-masonry beam", as shown in Figure 19.

"Short masonry-masonry beams" generally appeared in the mining process of RCN-P. The ultimate purpose of the support in the entry is to keep the structure stable, thereby improving the bearing capacity of the roof and maintaining the surrounding rock of the surrounding rock of the roadway.

4.4 Mechanical analysis

According to the results of microseismic monitoring and physical similarity simulation experiments, a short masonry-masonry structure mechanical model was formed as shown in figure 20, the figure is established with RCN-P mining.

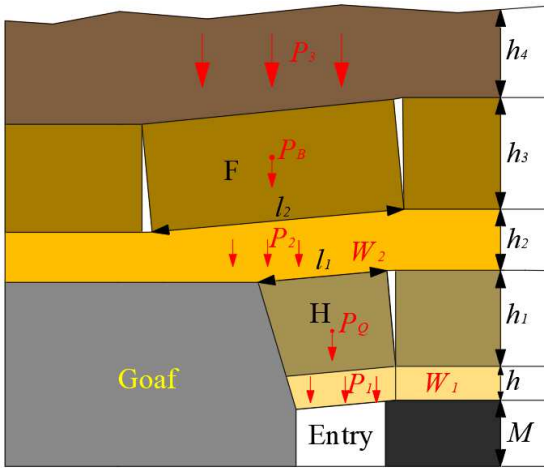

Figure. 20 Mechanical calculation model

In Figure 20, h_4 is the thickness of the upper rock layer of the basic roof key layer, h_3 is the thickness of the basic roof key layer, h_2 is the thickness of the weak layer, h_1 is the thickness of the roof cutting control layer, h is the thickness of the immediate roof, M is for mining height, l_2 is the length of the key block F, l_2 is the length of the key block H.

The roof stress of the entry include: W_1 is the immediate roof stress, P_1 is the stress of roof cutting control layer, P_Q is the weight of block F, W_2 is the stress of the weak layer, P_2 is the stress of basic roof key layer, P_B is the weight of block, P_3 is the effective stress transmitted by upper rock layer of the basic roof key layer.

1)Stress of basic roof key layer(as shown in figure 21)

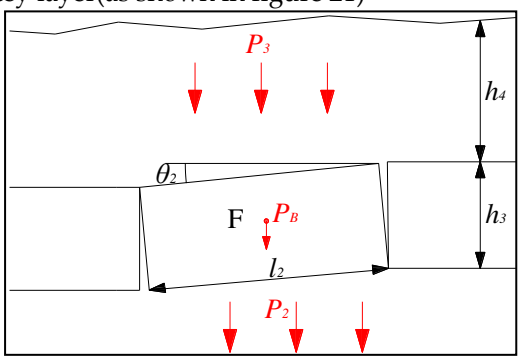

Figure.21 Mechanical calculation model for basic roof key stratum

$$P_3 = K_G l_2 \sum h_4 \gamma_2 \tag{1}$$

K_G is the load transfer coefficient[22], γ_2 is the bulk density of the loading layer.

$$K_G = \frac{l_2}{2h_3\lambda_3 \tan\varphi} \tag{2}$$

λ_3 is the lateral stress coefficient of the overlying rock above the basic roof, φ is the internal friction Angle.

$$P_B = l_2 \sum h_3 \gamma_1 \tag{3}$$

The hinged structure formed after the key layer of the basic roof is broken exists in the form of masonry beam. By introducing the calculation formula of masonry beam[23], the formula can be introduced.

$$P_2 = (l_2 \sum h_3 \gamma_1 + P_3)[\frac{4i_2 - 3\sin\theta_2}{2(2i_2 - \sin\theta_2)} - \frac{\tan\varphi_2}{i_2 - \sin\theta_2 + 2\sin\theta_2}] \tag{4}$$

γ_1 is the bulk density of bedrock, i_2 is the ratio of length to thickness of block F, θ_2 is the rotation angle of block F, φ_2 is the internal friction angle of bedrock.

2) Stress of the weak layer

The force of the weak rock formation is the weight of the overlying rock between the roof cutting control layer and the basic roof key layer, and it acts directly on the roof cutting control layer in the form of a load.

$$W_2 = l_1 \sum h_2 \gamma_2 \tag{5}$$

3)Stress of roof cutting control layer (as shown in Figure 22)

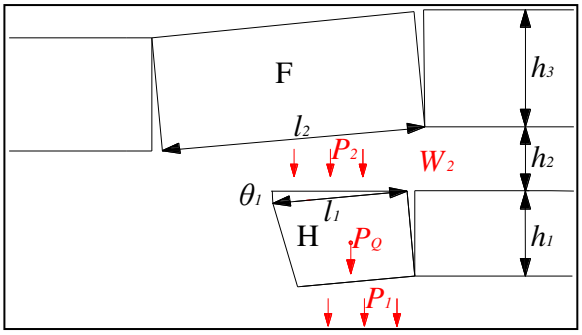

Figure.22 Mechanical calculation model for control key stratum

The hinge structure formed after the roof cutting control layer is destroyed is a short masonry beam structure[11]. The formula can be introduced.

$$P_Q = l_1 \sum h_1 \gamma_1 \tag{6}$$

$$P_1 = \frac{1.7 - (1.2 + 4.6 i_1) \tan \theta_1}{4 - 1.2 \tan \theta_1} (P_2 + W_2 + P_Q) \tag{7}$$

According to the formula (4)~(6):

$$P_1 = \frac{1.7 - (1.2 + 4.6 i_1) \tan \theta_1}{4 - 1.2 \tan \theta_1} (l_1 \sum h_1 \gamma_1 + P_2 + l_1 \sum h_2 \gamma_2) \tag{8}$$

i_1 is the ratio of length to thickness of block H, θ_1 is the rotation angle of block H.

4) Stress of immediate roof

$$W_1 = l_1 \sum h \gamma_2 \tag{9}$$

To sum up, it is determined that the minimum support resistance R to keep the roof stable by RCN-P mining is:

$$R \geq l_1 \sum h \gamma_2 + \frac{1.7 - (1.2 + 4.6 i_1) \tan \theta_1}{4 - 1.2 \tan \theta_1} [l_1 \sum h_1 \gamma_1 + P_2 + l_1 \sum h_2 \gamma_2] \tag{10}$$

5. Conclusions

(1)As can be seen from the microseismic detection results with RCN-P mining in thick coal seam, the horizontal distribution of microseismic events is featured by "two zones and one line", namely, the horizontal direction is divided into crack generation area and roof movement area, which are located 0-25m ahead of and 0-32m behind the mining face, respectively. The microseismic events, 4-8m within the coal wall side of the entry in the inclined direction, are linearly distributed, where lays the secondary lateral breaking line.

(2) The vertical distribution of roof microseismic events with RCN-P mining is basically featured by "three zones." The crack generation area and the roof movement area are located 0-12m and 13-45m above the entry, respectively, with the latter being the main area of the entry roof breaking movement and the crack development area being more than 50m above the entry.

(3) Periodic characteristics of microseismic events are obvious. Few microseismic events are distributed in the leading position in the initial stage of the period weighting. A concentrated event of microseisms occurred in the leading position of the working face in the middle stage, forming a leading macroscopic crack, expanding continuously. The distribution range, intensity and frequency of microseismic events reach the maximum, and basic roof reaches the limit breaking state in the final stage. Compared with the normal mining, the RCN-P mining reduces the periodic weighting length by 10.2%, and the pressure strength is increased by 11%.

(4) As is shown from the actual measurement and simulation results, the rock formations controlling the roof movement with RCN-P mining include: the basic roof key layer located within the roof movement area and outside the cutting height range, and the roof cutting control layer located in the crack generation zone within the height of the roof cutting area, which has a bearing function. The thickness of roof cutting control layer is mainly affected by the cut parameters. Shorter cutting roof height indicates less thickness of the cutting roof control layer and weaker bearing capacity of the "small structure." The great height of roof cutting predicts the increasing thickness of the roof cutting control layer and the enhancing bearing capacity, which effectively realizes the bearing of the overlying rock mass.

(5) The breaking and rotation of the basic roof key layer formed the basic roof side triangular arch structure, with the basic broken roof being featured by "masonry beam" structure of the key block. It is easy to cut and break along the coal wall when the roof cutting control layer cannot bear the force of the overlying surrounding rock. The breaking position is the lateral breaking line of microseismic monitoring, forming a "short masonry" structure, forming a "short masonry beam-masonry beam" structure with the basic roof. Through mechanical analysis, the structure model is established, the mechanical analysis is conducted, and the calculation method to the roof-stablility minimum supporting resistance in the entry is obtained.

Author Contributions: Conceptualization, L.Z.; Experimental Design, M.Z. and Q.H.; Validation, L.Z. and M.Z.; Theoretical Analysis, Q.H. and M.Z.; Data Curation, K.X.; Supervision, Y.W.; Writing—Original Draft Preparation, M.z; Writing—Review & Editing, L.Z. and W.G. Supervision, M.Z.; Project Administration, L.Z.; Funding Acquisition, L.Z.

Funding: This research was funded by the National Natural Science Foundation of China, grant number No.51674190.

Acknowledgments: We thank the National Natural Science Foundation of China for its support of this study. We thank the academic editors and anonymous reviewers for their kind suggestions and valuable comments.

Conflicts of Interest: The authors declare no conflict of interest.

References

1. He,M.C.; Song,Z.Q.; Wang,A.; Yang,H.H.; Qi,H.G.; Guo,Z.B. Theory of longwall mining by using roof cutting shortwall team and 110 method—the third mining science and technology reform.*J. Coal science & technology magazine*, **2017**,13,1-9.
2. He,M.C.; Zhang,G.F.; Yu,X.P. Research on the technique of no-pillar mining with gob-side entry formed by advanced roof caving in the protective seam in Baijiao Coal Mine.*J. Journal of Ming & Safety Engineering,* 2011,21,511~516.
3. Zhen,E.Z.; Wang,Y.J.; Yang,J; He,M.C.; Comparison of the macroscopical stress field distribution characteristics between a novel non-pillar mining technique and two other current methods.*J. Advances in Mechanical Engineering*. **2019**,5,1-15.
4. Liu,T.C. Application and Development in maintaining roadways without chain pillars.*J. Ground Pressure and Strata Control*. **1994**,4.
5. Yang,X.J.; Wang,E.Y.; Ma,X.G.; Zhang,G.F.; Huang,R.F.; Lou,H.P. A case strdy on optimization and control techniques for entry stability in non-pillar longwall mining.*J. Energie*s. **2019**.12.291-308.
6. Mahdevari, S.; Shahriar, K.; Sharifzadeh, M.; Tannant, D.D. Stability prediction of gate roadways in longwall mining using artificial neural networks. *Neural Comput*. Appl.2017,28,3537-3555.
7. Huang,Q.X.; Zheng,C. Theory of self-stable ring in roadway support.*J. Rock and Soil Mechanics*, **2016**,37,1231-1236.
8. Huang,Q.X.; Zhao,M.Y.; Zhang,Q.F.; Shao,S.C.; Ma,K.S. Mechanisms of outward dislocation sliding of roadway sides and its support in a thick coal seam with a soft mudstone interlayer.*J. Rock and Soil Mechanics*, **2016**,37,2353-2358.
9. Song,Z.Q.; Cui,Z.D.; Xia,H.C.; The fundemental theoretial and engineering research on the green safe no coal pillar mining model by mainly using coal gangue backfill.*J. Journal of China Coal Society*, **2010**,35,705~710
10. Qian, M.G. On sustainable coal mining in China. *J. China Coal Soc*. **2015**, 35, 529-534.

11. Qian, M.G.; Xu, J.L.; Wang, J.C. Further on the sustainable mining of coal. *J. China Coal Soc.* **2018**, 43, 1-12.
12. Li,S.; Li,J.W.; Fan,C.J.; Luo,M.K.; Han,Y.L. Roof subsidence laws and control technology for gob-side entry retaining in fully-mechanized top-coal caving face.*J. Journal of China Coal Society*, **2015**,40,1989-1994.
13. He,M.C.; Gao,Y.B.; Yang,J.; Gong,L.W.; An innoavtive approach for gob-side entry retaining in thick coal seam longwall mining .*J. Energies,* **2017**,10.1785-1807.
14. Zhu,Z.; He,M.C.; Wang,Q.; Gao,Y.B.; Wang,Y.J.; An innovative non-pillar mining method for gateroad formation automatically and its application in Ningtiaota coal mine.*J. Journal of China University of Mining & Technology*. **2019**,48
15. Hu,J.Z.; He,M.C.; W,J.; Ma,Z.M.; W,Y.J.; Zhang,Y.X. Key parameters of roof cutting of gob-side entry retaining in a deep inclined thick coal seam with hard roof.*J. Energies*, **2019**,12,934-953.
16. Liu.X.; Hua X.Z.; Yang,P.; Huang,Z.G.; A study of the mechanical structure of the direct roof during the whole process of non-pillar gob-side entry retaining by roof cutting.*J. Energy exploration*, **2020**,0,1-19 .
17. Hua,X.Z.; Zhang,D.L.; Research on supporting technology of gob-side entry retaining in the deep mining .J. **2009**,2,4~38.
18. Zhang,N.; Yuan,L.; Han,C.L.; Xue,J.H.; Kan,J.G. Stability and deformation of surrounding rock in pillarless gob-side entry retaining.*J. Safety Science*, **2012**,50,593-599.
19. Zhang Nong, Han Changliang, Kan Jiaguang. Theory and practice of surrounding rock control for pillarless gob-side entry retaining.*J. Jouranl of China Coal Society*, **2014**,39(8):1635-1641
20. Li,L.F.; Li,G.; Gong,W.L.; Wang,J.; Deng,H.L. Energy evolution pattern and roof control strategy in non-pillar mining method of goaf-side entry retaining by roof cutting- a case study.*J. Sustainability*. **2019**,11,7029-7048.
21. Luan,H.J.; Jiang,Y.J.; Lin,H.L.; Li,G.F.; Development of a new gob-side entry-retaining approach and its application.*J. Sustainability*. **2018**,10,470-485.
22. Huang,Q.X. Ground pressure behavior and definition of shallow seams.*J. Chinese Journal of Rock Mechanics and Engineering*. **2002**, 21,1174-1177.
23. Huang,Q.X.; Zhao,M.Y.; Huang,K.J.; Study of Roof Double Key Strata Structure and Support Resistance of Shallow Coal Seams Group Mining.*J. Journal of China University of Mining & Technology*. **2019**,48,71-77.
24. K. Ma a,b,c,*, X.Y. Sun a,b, C.A. Tang a,b, F.Z. Yuan a,b, S.J. Wang d, T. Chen. Floor water inrush analysis based on mechanical failure characters and microseismic monitoring.*J.* 2021.108
25. Mikkelsen PE, Green GE. Piezometers in fully grouted boreholes. In: Symposium on Field Measurements in Geomechanics. Oslo, Norway: FMGM 2003; **2003**. September:A.A. Balkema
26. Guo,R.P. Influence of the interval length of hydraulic packer systems on thermally-induced pore pressure measurements in rock.J. International Journal of Rock Mechanics & Mining Sciences. **2020**.135. 1-9.
27. Wang,S.C.; Dou,L.M.; Wang,Z.Y.; Bai,J.Z.; Chai,Y.J.; Mechanism of Coal Bursts Induced by Horizontal Section Mining of Steeply Inclined Coal Seams and Application of Microseismic Multiparameter Monitoring in Early Warning.*J. Advances in civil engineering*. **2020**.
28. Wang,J.W.; Wang,S.B.; Yang,J.; Wang,Q.; Ma,L.L.; He,M.C. Roof failure mechanism of gob-side entry retaining by roof cutting and pressure releasing and its control technology.*J. Coal Science and Technology*. **2017**.8.80-84.

Figures

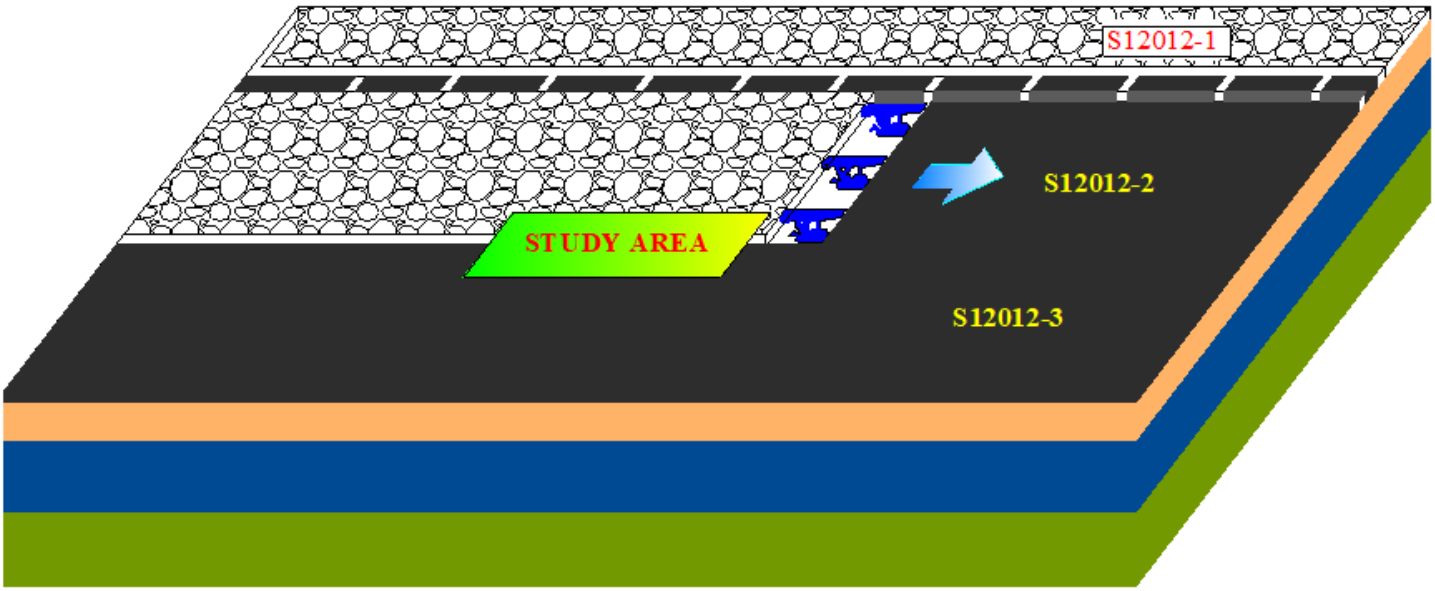

Figure 1

Study area layout

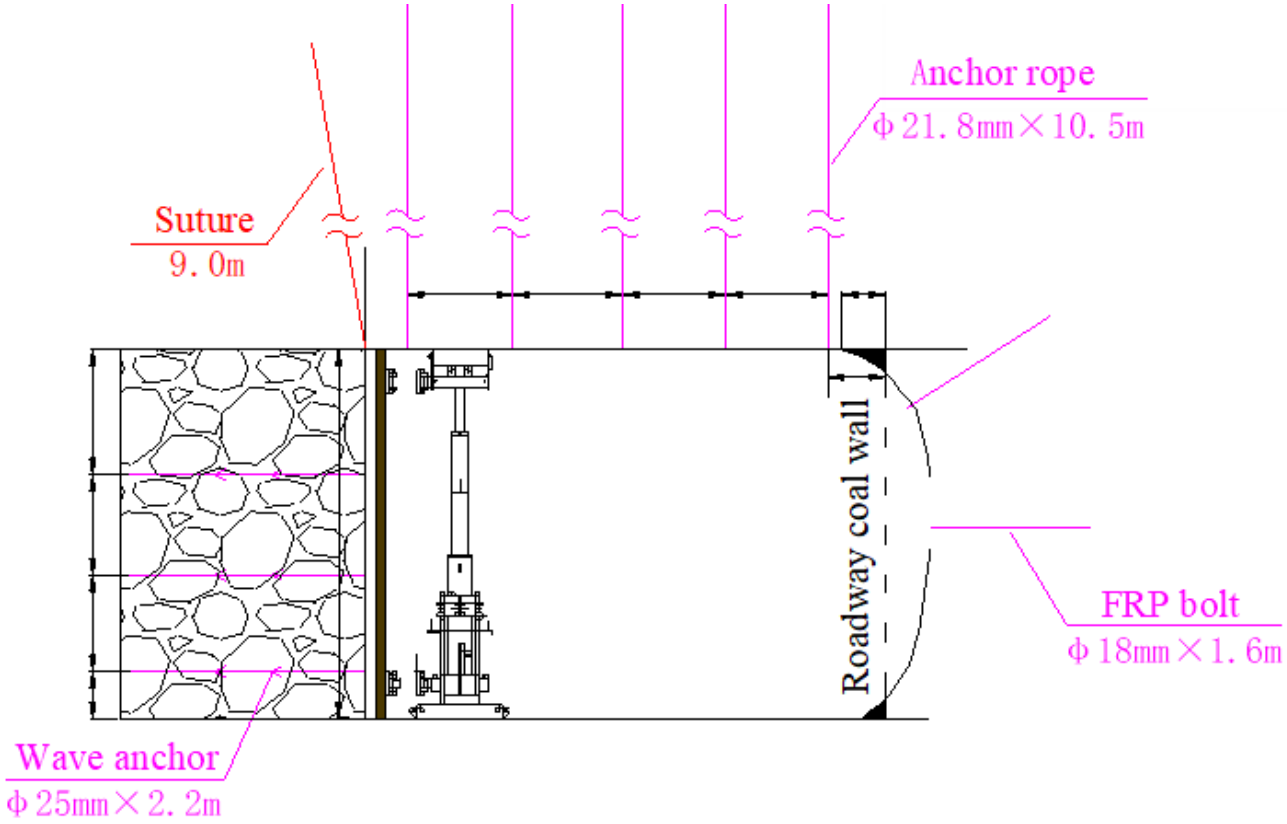

Figure 2

Layout of entry section

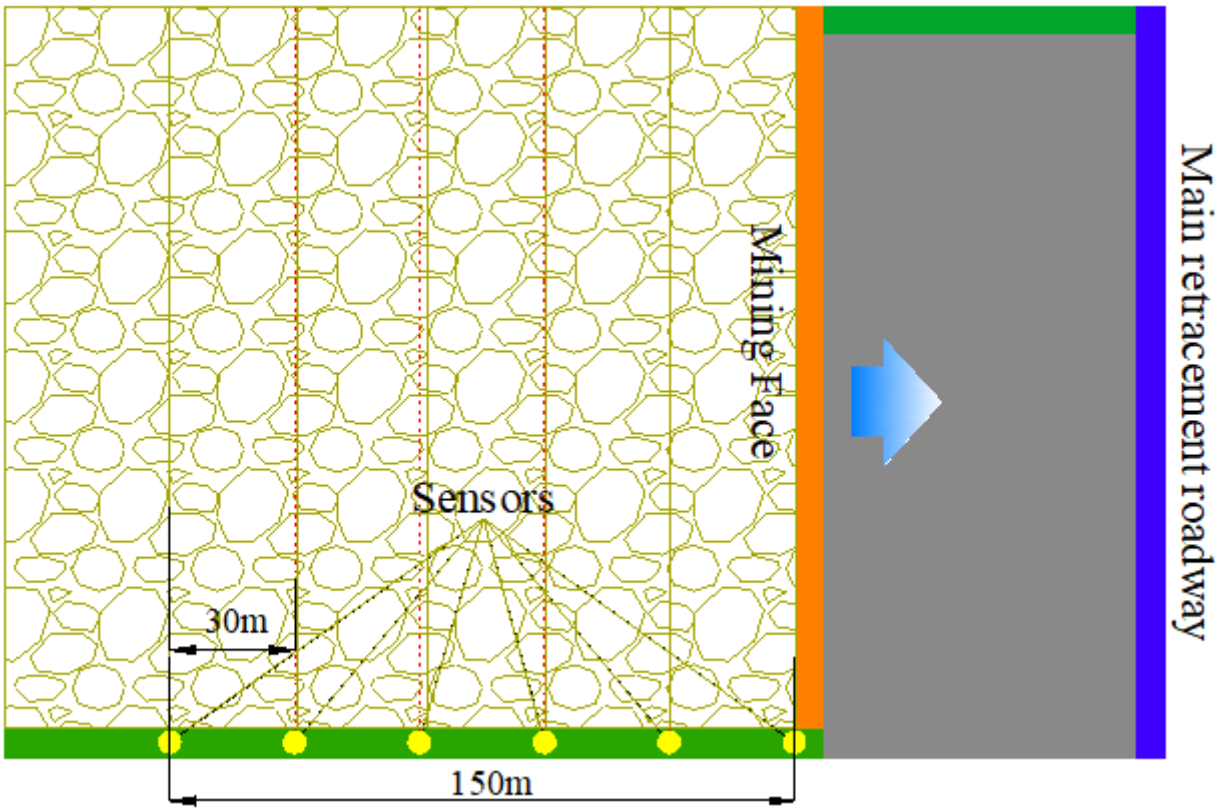

Figure 3

Top view of microseismic sensor measuring point layout

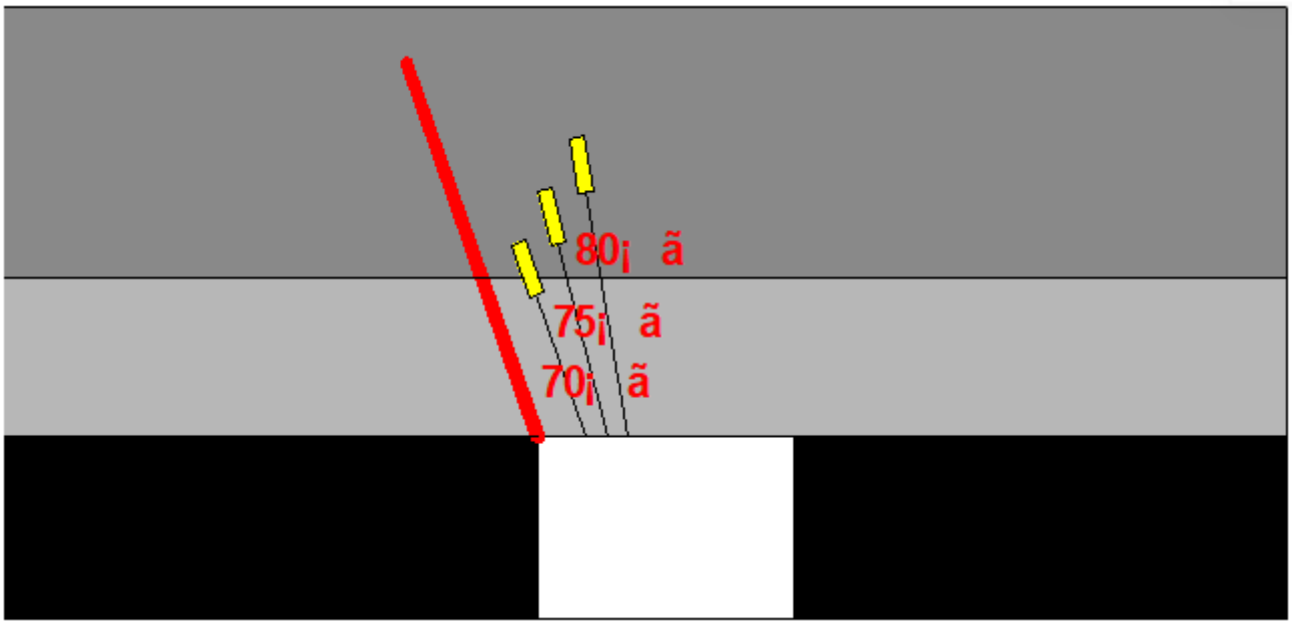

Figure 4

Side view of microseismic sensor layout

Figure 5

Drilling installation construction

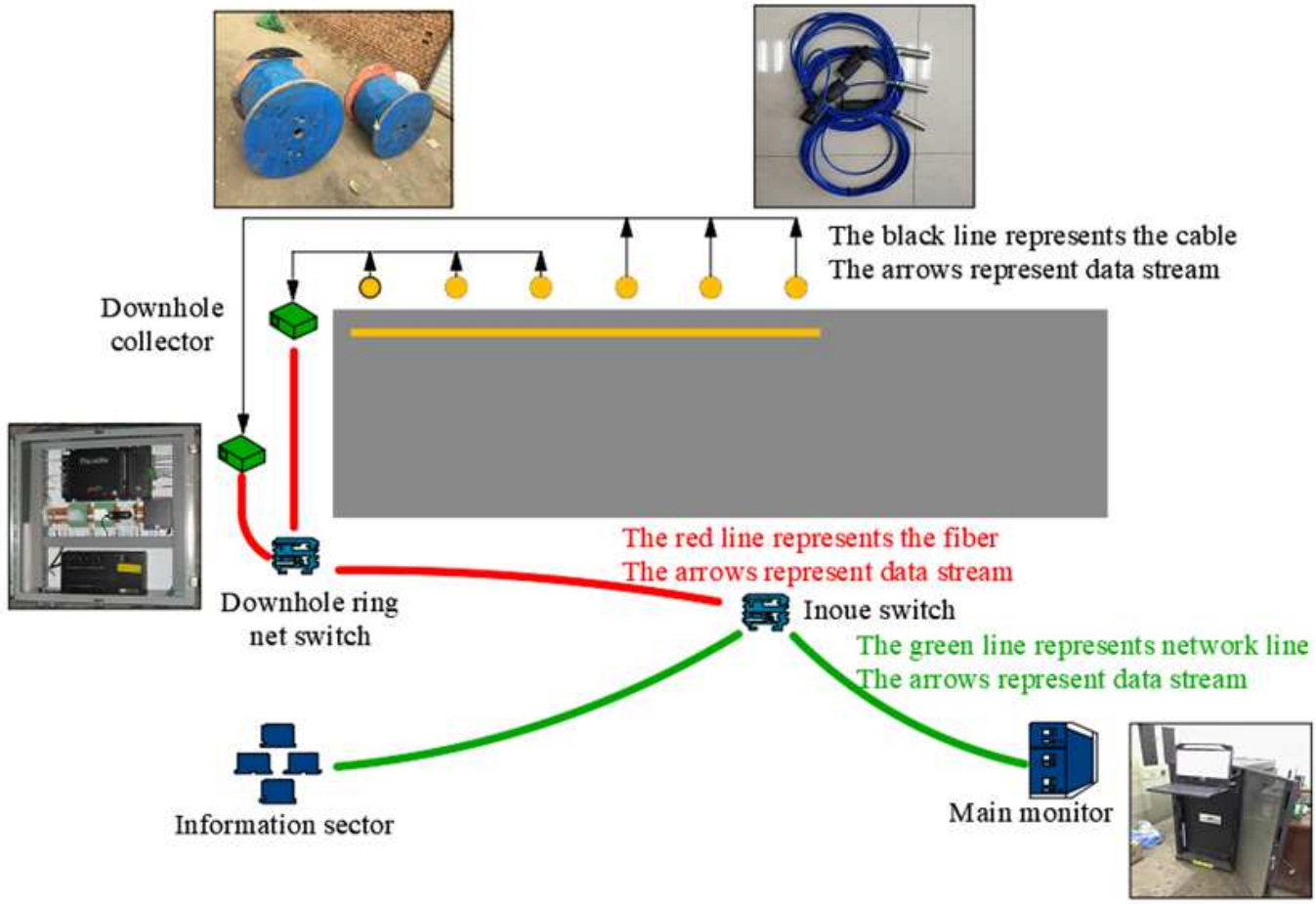

Figure 6

Communication Line Layout

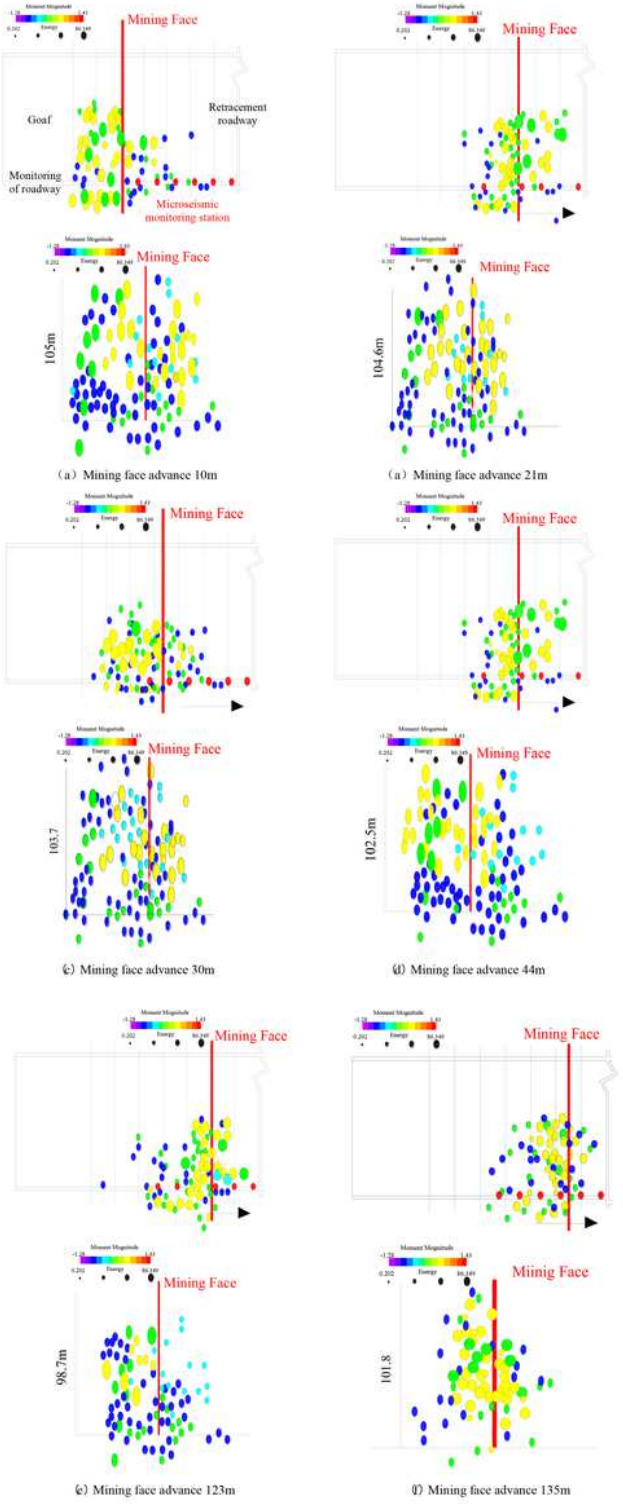

Figure 7

Distribution characteristics of microseismic events at mining face

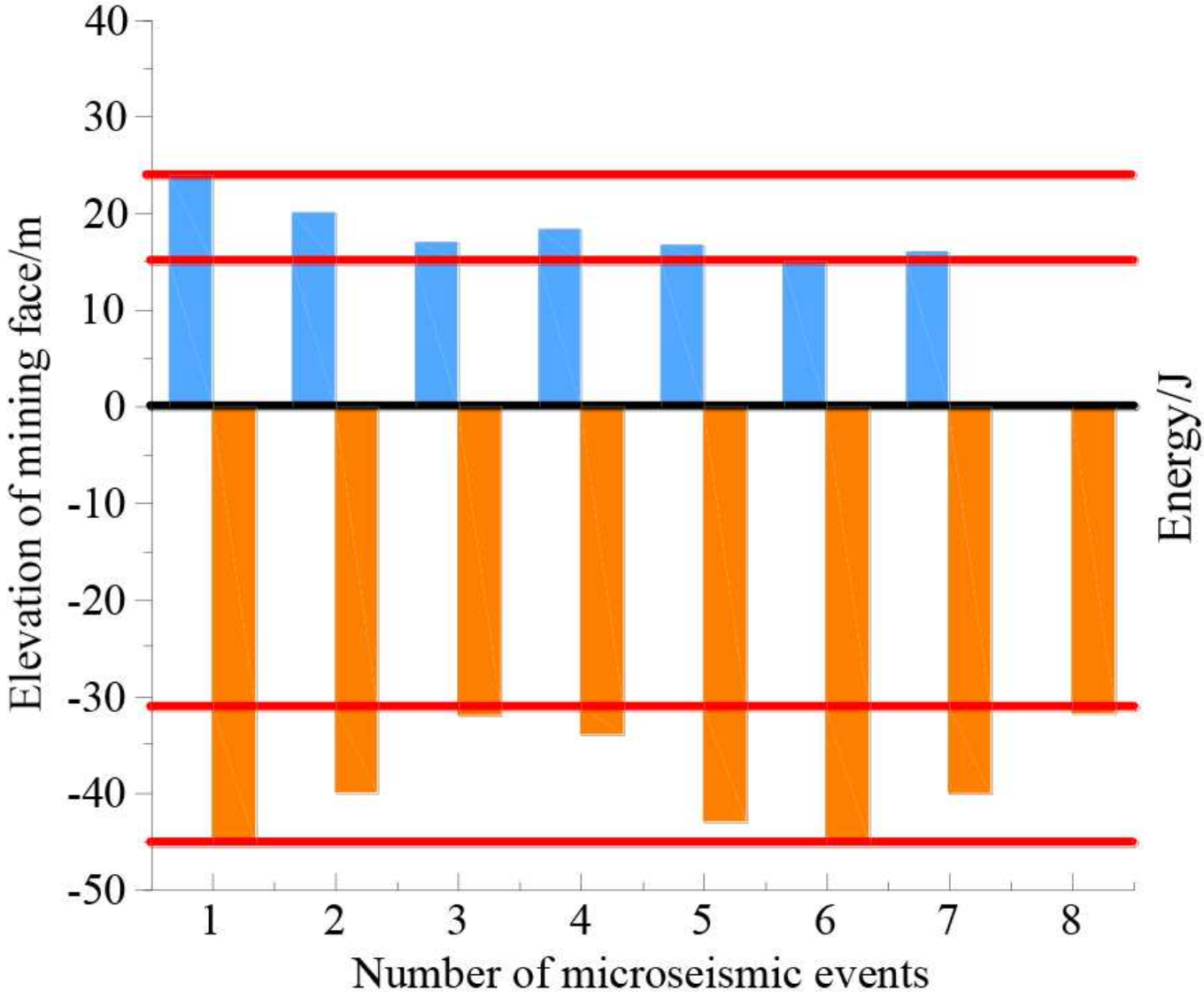

Figure 8

The impact range

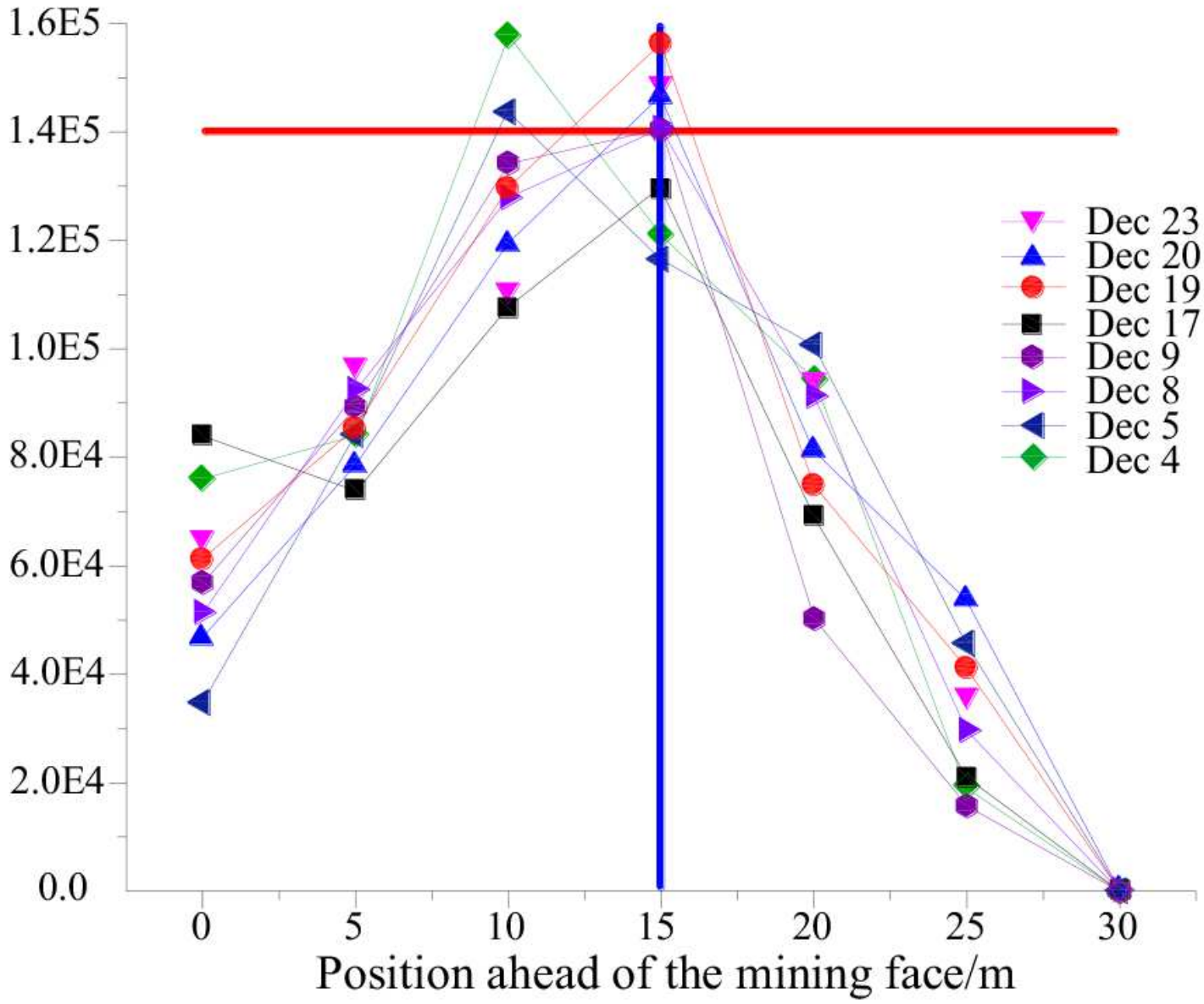

Figure 9

Energy distribution curve

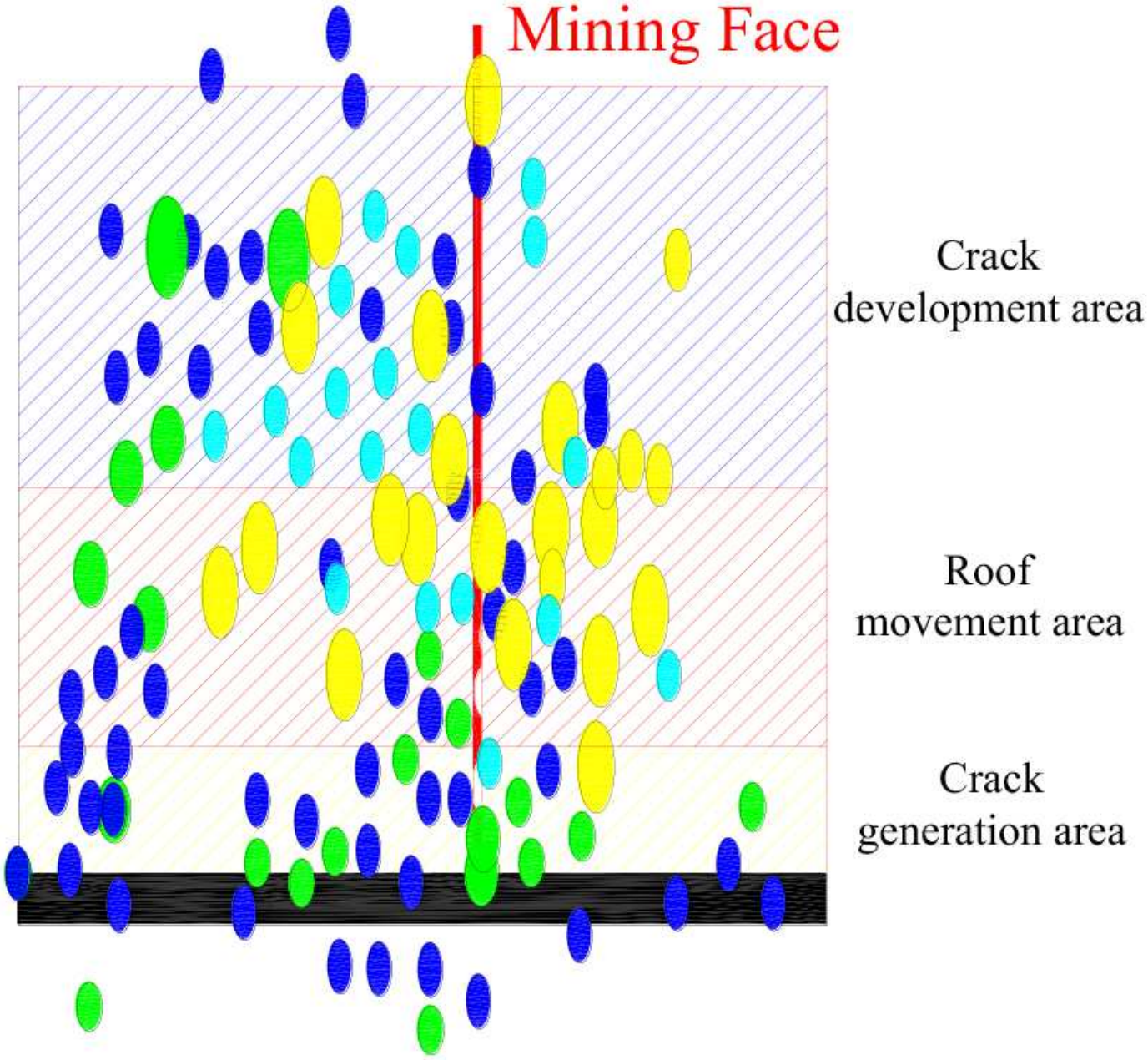

Figure 10

Vertical distribution characteristics

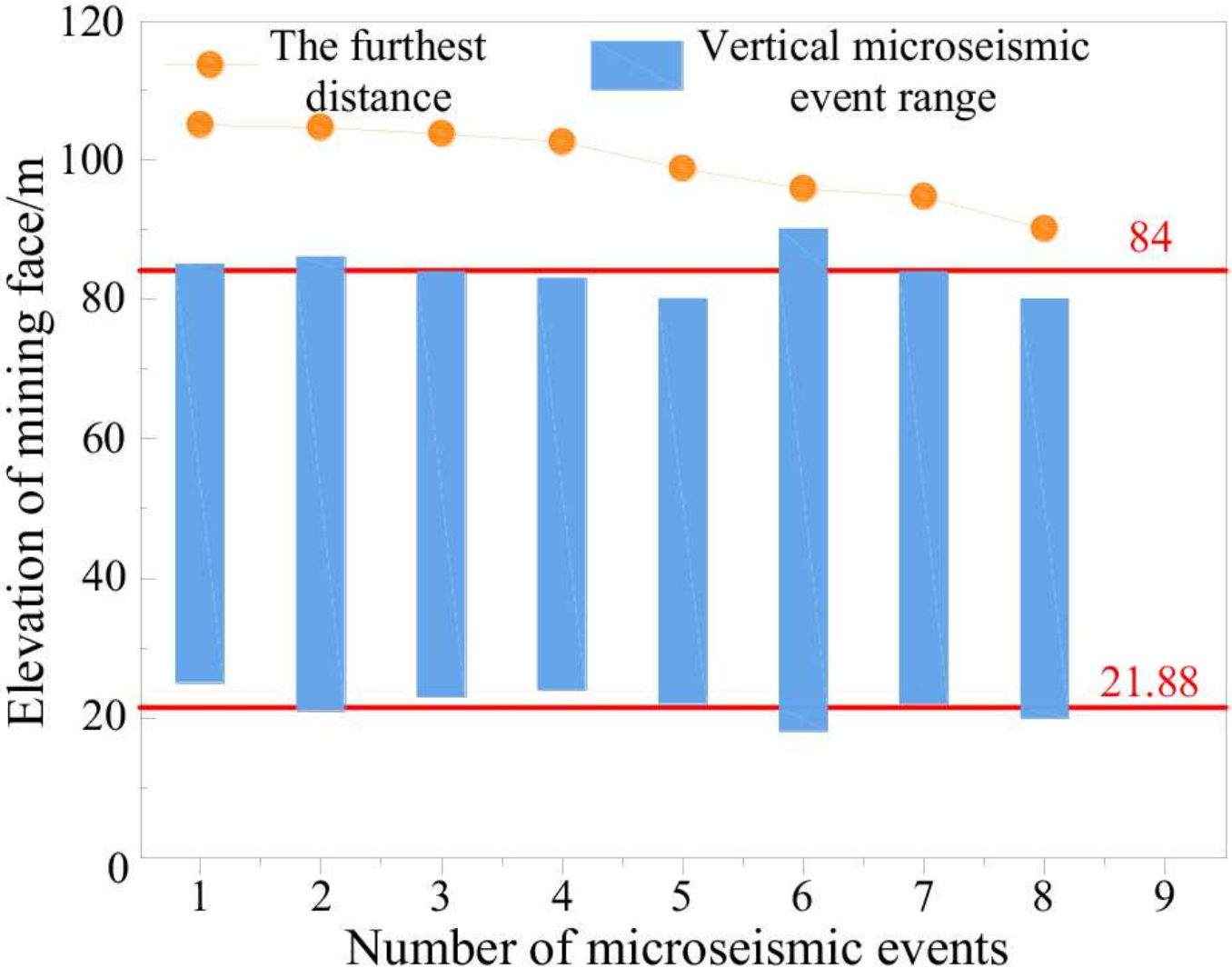

Figure 11

Vertical concentration range

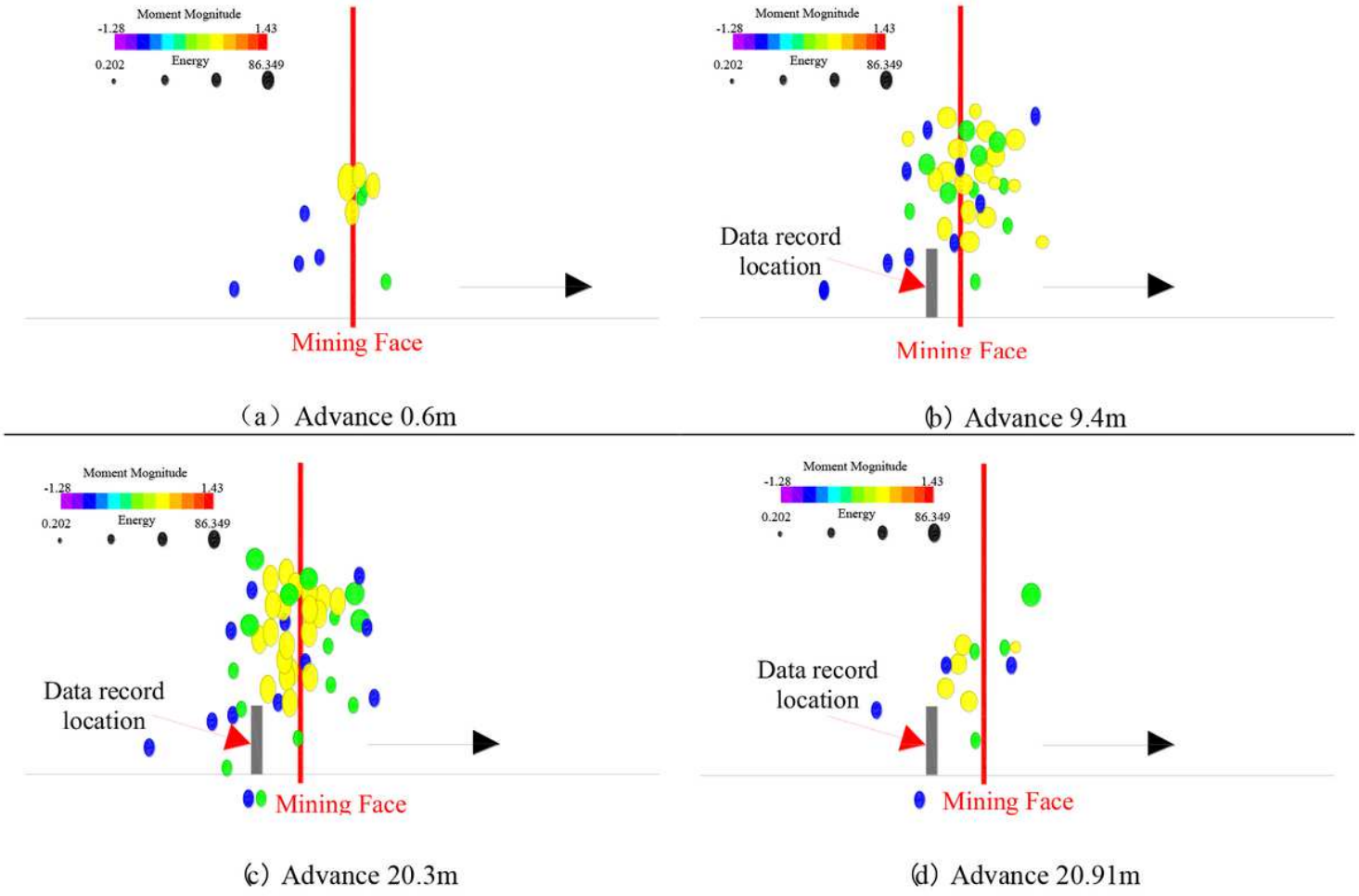

Figure 12

Period distribution characteristics of microseismic events

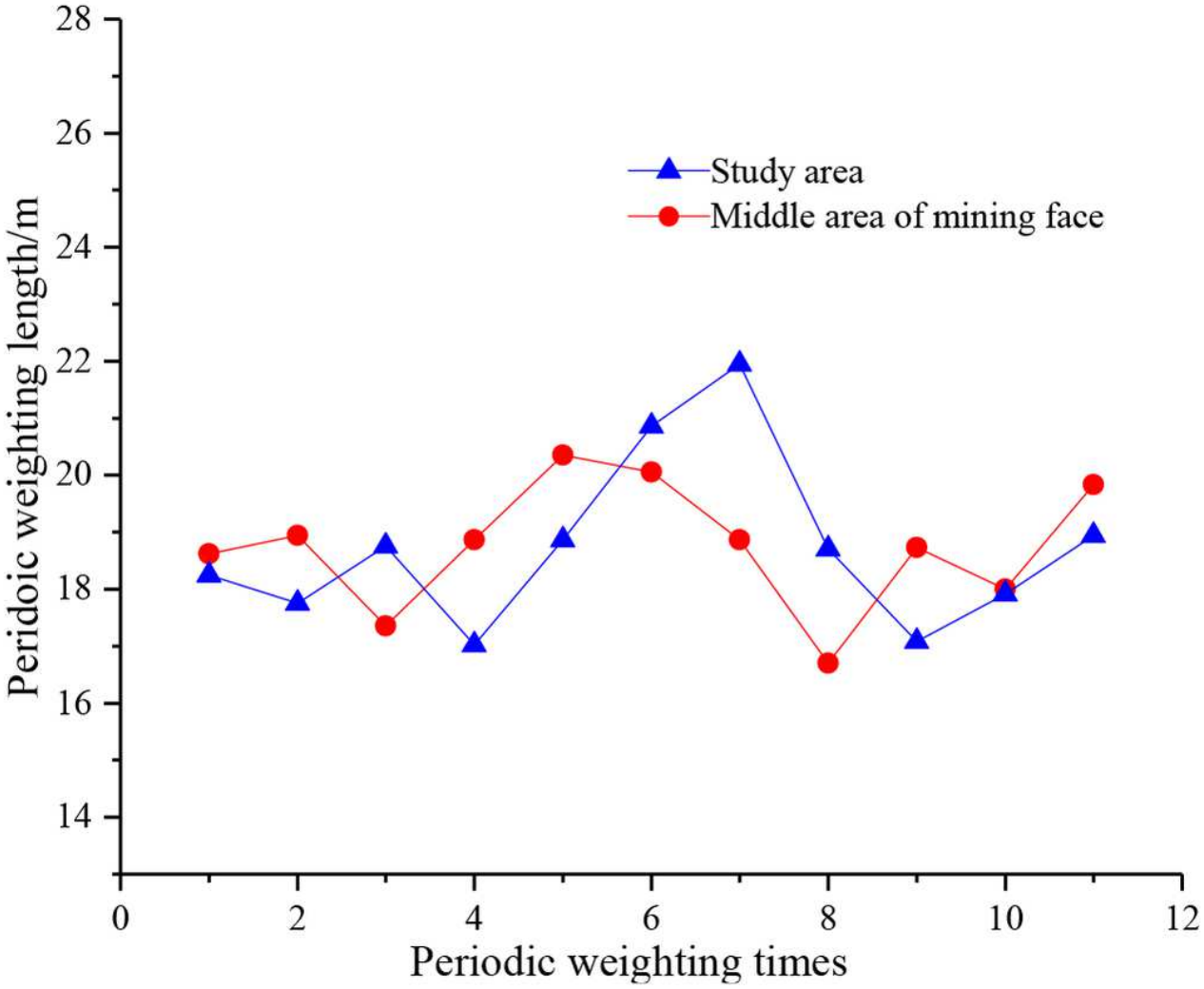

Figure 13

Periodic weighting length of microseismic monitoring

Figure 14

Physical simulation panorama

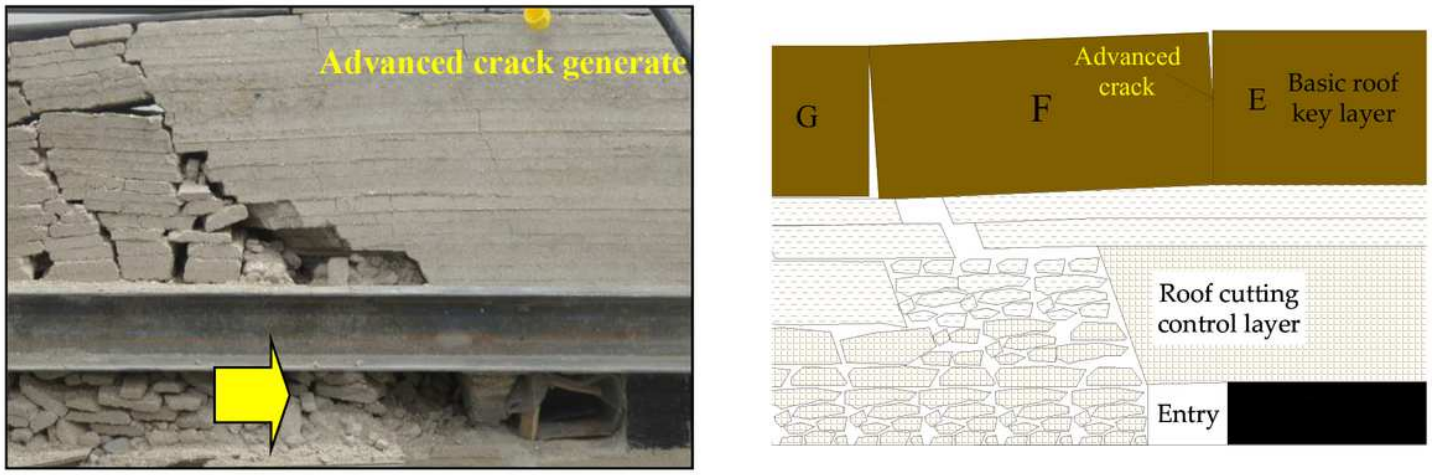

(a) Similarity simulation experiment results (b) Structural diagram

Figure 15

Triangular arch structure of Basic roof

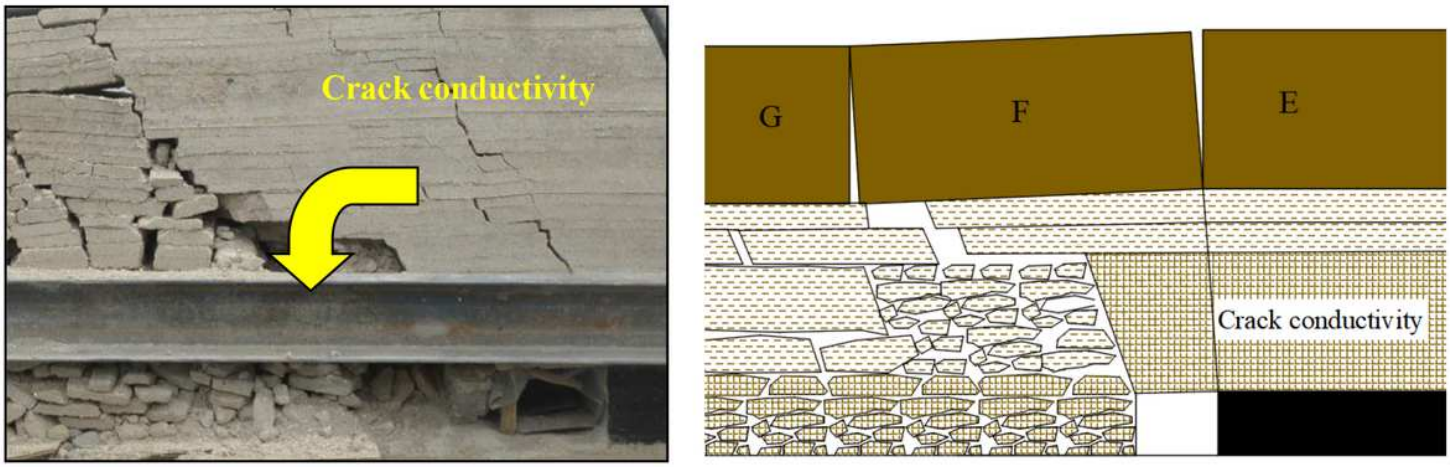

(a) Similarity simulation experiment results

(b) Structural diagram

Figure 16

The roof cutting control layer breaking

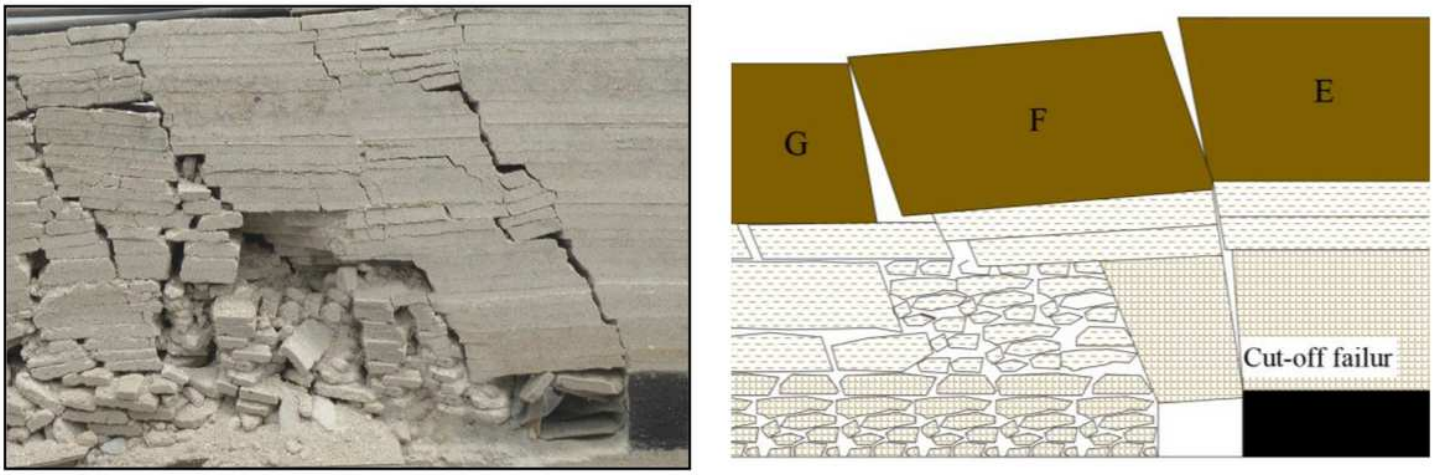

(a) Similarity simulation experiment results

(b) Structural diagram

Figure 17

Cut-off failure of roof

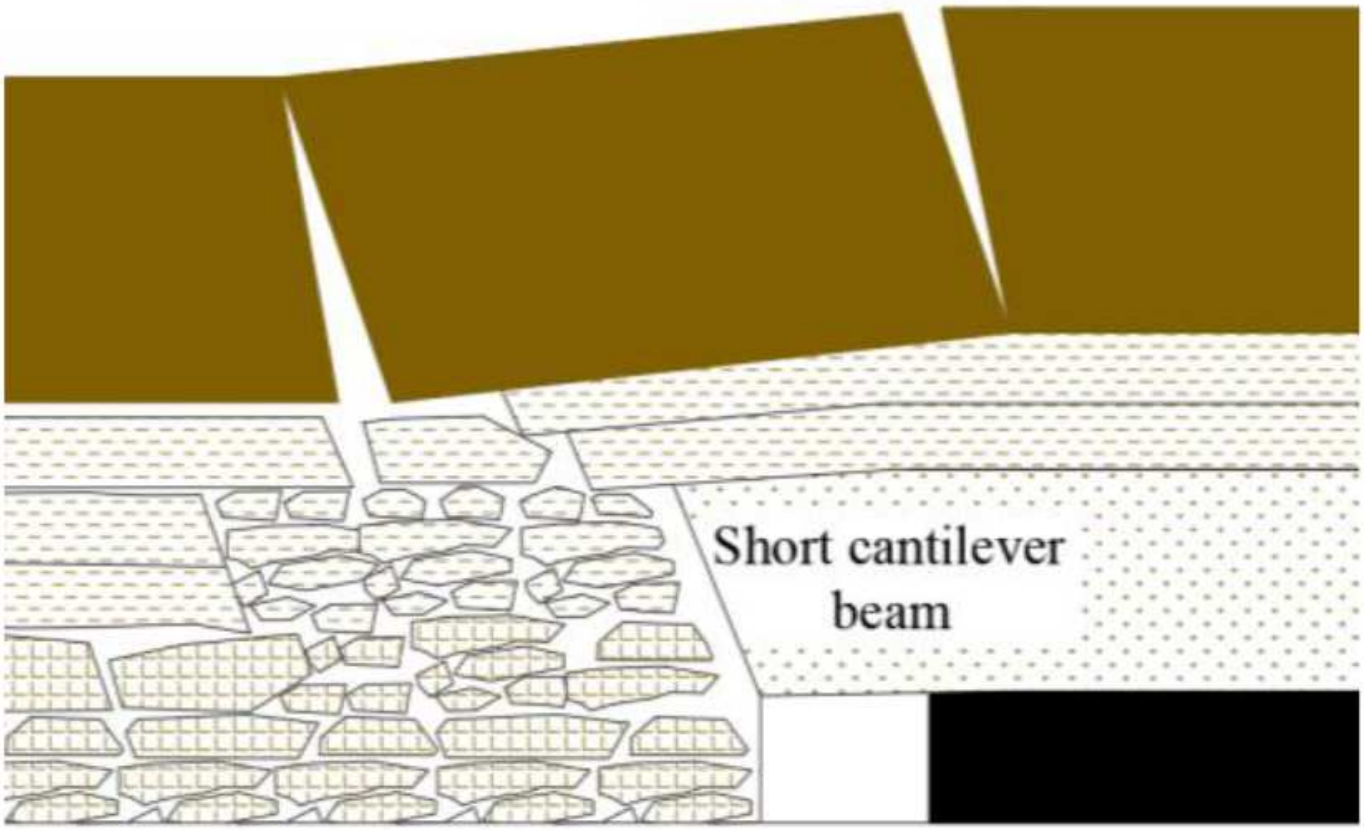

Figure 18

"Short cantilever beam - masonry beam" structure

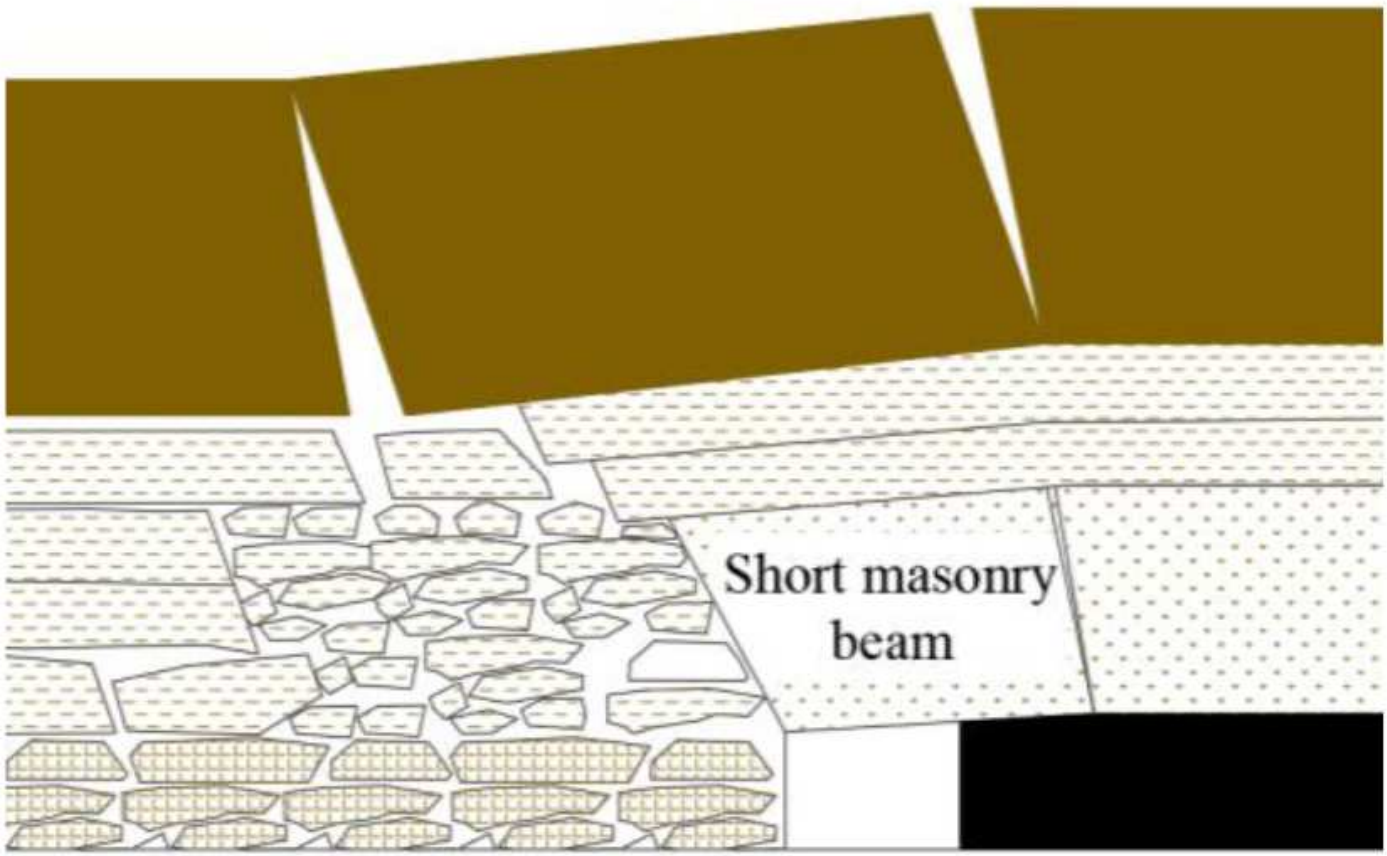

Figure 19

"Short masonry beam - masonry beam" structure

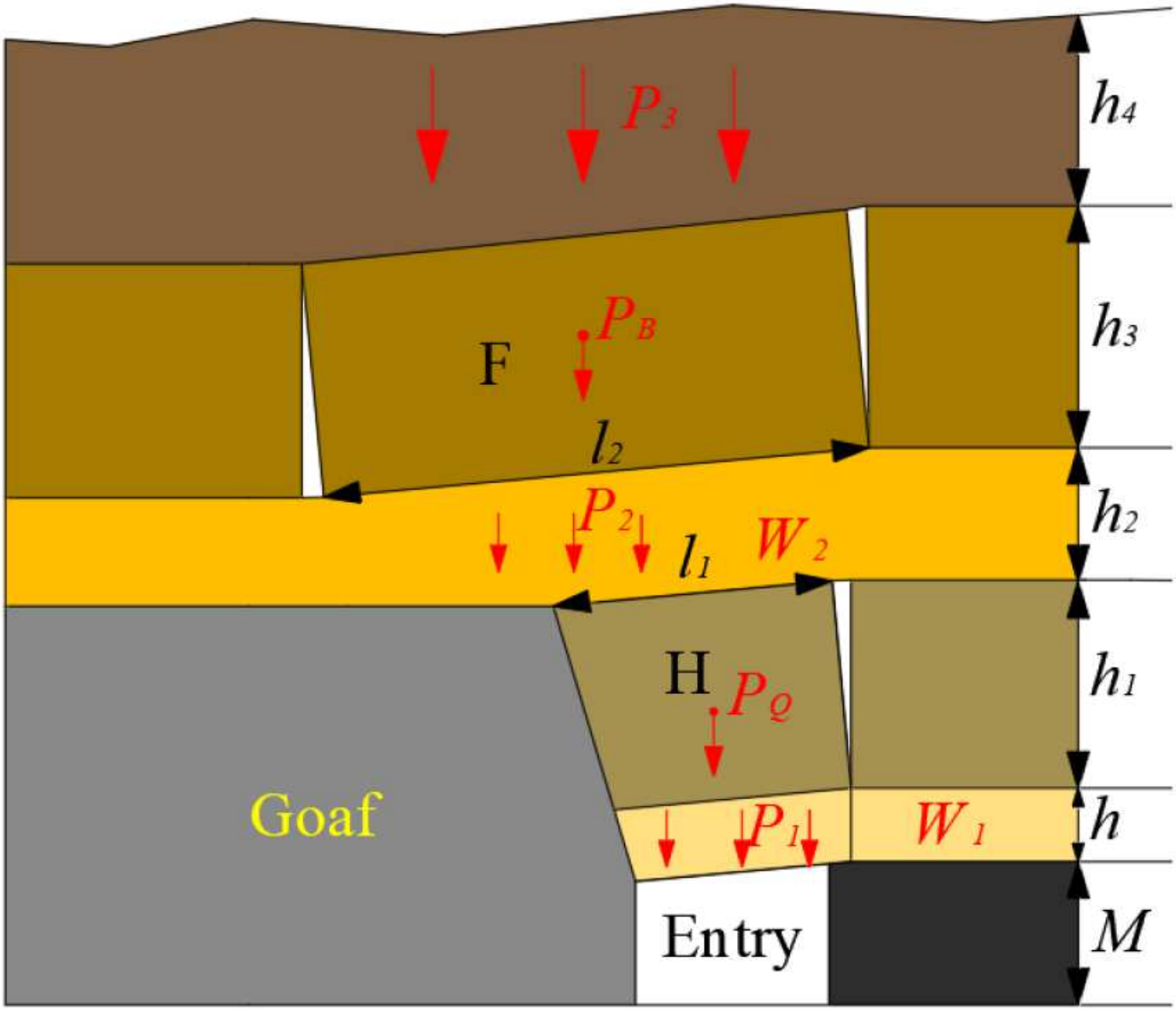

Figure 20

Mechanical calculation model

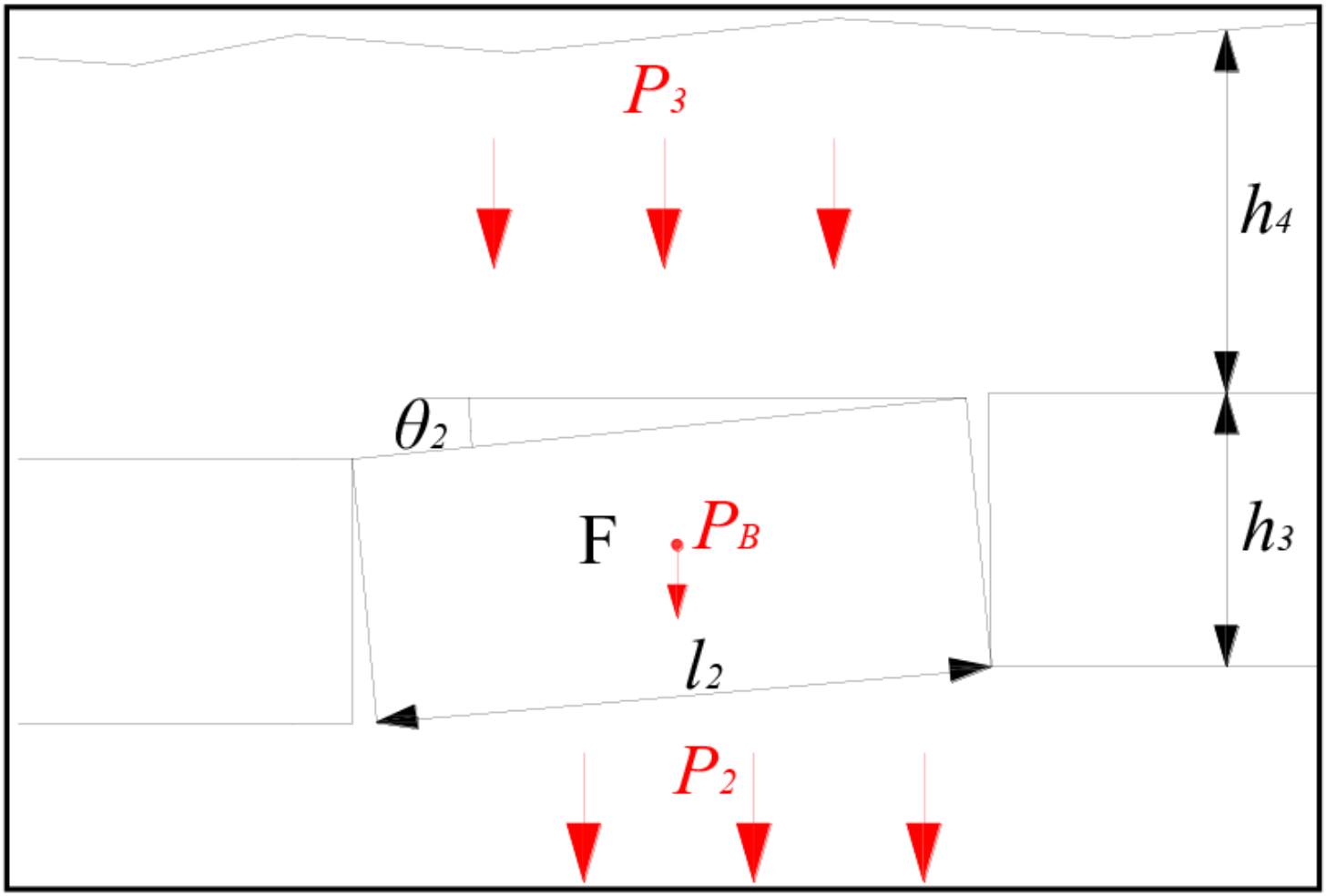

Figure 21

Mechanical calculation model for basic roof key stratum

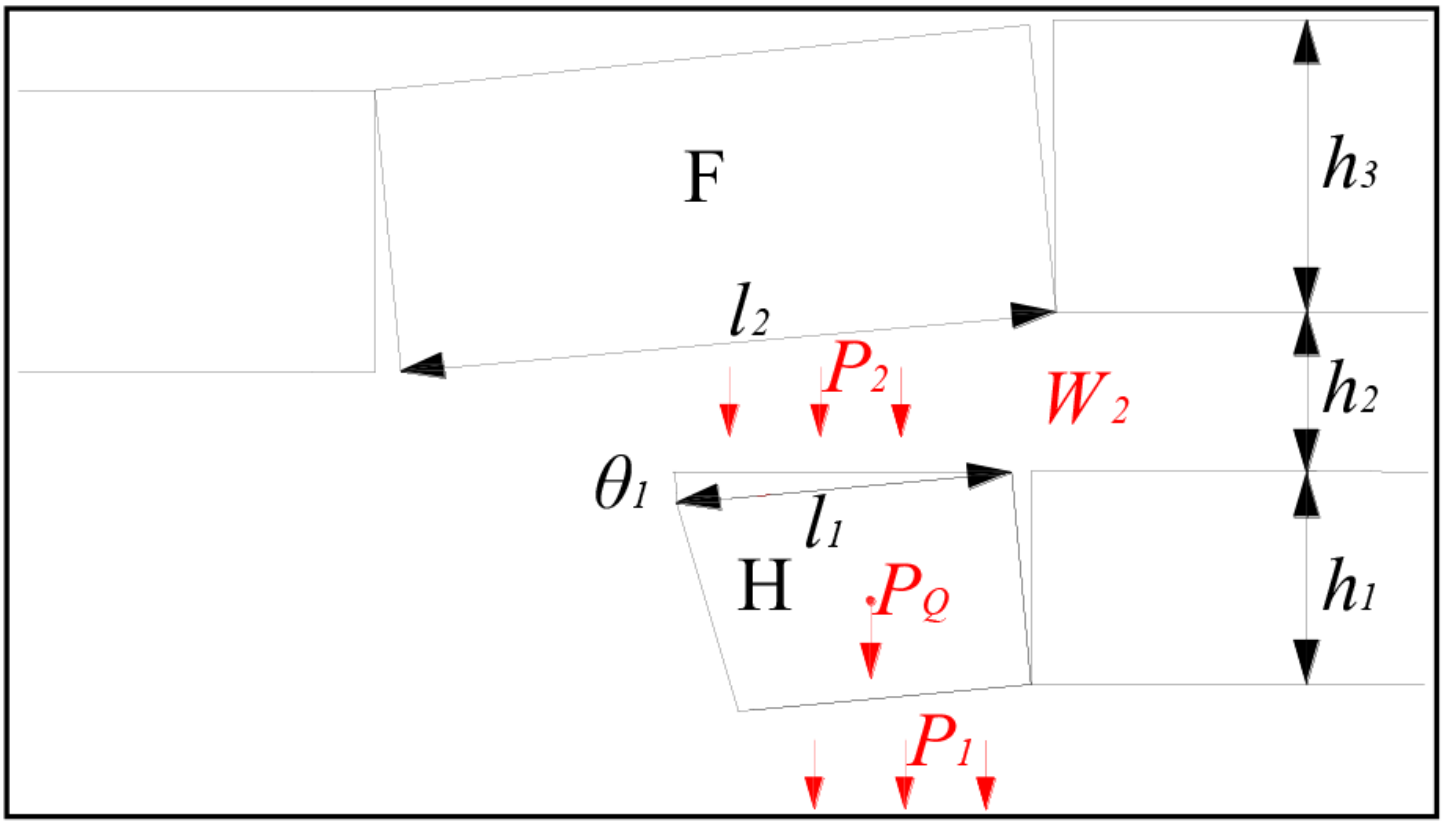

Figure 22

Mechanical calculation model for control key stratum